P-04-208

Oskarshamn site investigation

Drill hole KSH01A

Triaxial compression test of intact rock

Lars Jacobsson
SP Swedish National Testing and Research Institute

May 2004

Svensk Kärnbränslehantering AB
Swedish Nuclear Fuel
and Waste Management Co
Box 5864
SE-102 40 Stockholm Sweden
Tel 08-459 84 00
+46 8 459 84 00
Fax 08-661 57 19
+46 8 661 57 19

ISSN 1651-4416
SKB P-04-208

Oskarshamn site investigation

Drill hole KSH01A

Triaxial compression test of intact rock

Lars Jacobsson
SP Swedish National Testing and Research Institute

May 2004

Keywords: Rock mechanics, Triaxial compression test, Elasticity parameters, Stress-strain curve, Post-failure behaviour.

Abstract

Triaxial compression tests with constant confining pressure, containing the complete loading response beyond compressive failure, so called post-failure tests, were carried out on 13 water saturated specimens of intact rock from borehole KSH01A in Simpevarp. The cylindrical specimens were taken from drill cores at three depth levels ranging between 299–322 m, 481–492 m and 708–714 m. Moreover, the rock types were Quarz monzodiorite (299–322 m and 708–714 m) and Fine-grained dioritoid (481–492 m). The elastic properties, represented by the Young's modulus and the Poisson ratio, and the compressive strength were deduced from these tests. The wet density of the specimens was determined before the mechanical tests. The specimens were documented by photographing the specimens before and after the mechanical testing.

The measured densities for the water saturated specimens were in the range 2,770–2,870 kg/m^3, which yields a mean value of 2,817 kg/m^3. Three confining pressure levels were used, 2, 7 and 10 MPa, and the peak values for the axial compressive stress were in the range 181.6–289.6 MPa. The elastic parameters were determined at load corresponding to 50% of the failure load and it was found that Young's modulus was in the range 67.1–89.2 GPa with a mean value of 76.8 GPa and the Poisson ratio was in the range of 0.17–0.24 with a mean value of 0.21. It should be remarked that some results have been excluded in the summary above as some specimens contained defects (cracks) and a few data were judged to be not representative for the homogenous rock material. Furthermore, it was seen from the mechanical tests that the material in the specimens responded in a brittle way.

Contents

1 Introduction

Triaxial compression tests, with loading beyond the failure point into the post-failure regime, have been conducted on water-saturated specimens sampled from borehole KSH01A in Simpevarp, see map in Figure 1-1. These tests belong to one of the activities performed as part of the site investigation nearby Oskarshamn lead by Swedish Nuclear Fuel and Waste Management Co (SKB). The tests were carried out in the material and rock mechanics laboratories at the department of Building Technology and Mechanics at Swedish National Testing and Research Institute (SP). All work is carried out in accordance with the activity plan AP PS 400-03-066 (SKB internal controlling document) and is controlled by SP-QD 13.1 (SP internal quality document).

SKB supplied SP with rock cores and they arrived at SP in May 2003 and were tested during March 2004. Cylindrical specimens were cut from the cores and selected based on the preliminary core logging with the strategy to primarily investigate the properties of the dominant rock type. The method description SKB MD 190.003, (SKB internal controlling document) was followed both for the sampling and for the triaxial compression tests and the method description SKB MD 160.002, (SKB internal controlling document) was followed when the density was determined. As to the specimen preparation, the end surfaces on the specimens were grinded in order to comply with the required shape tolerances and then put in water and kept stored in water, with a minimum of 7 days, up to testing. This yields a water saturation, which is intended to resemble the in-situ moisture condition. The density was determined on each specimen and the triaxial compression tests were carried out at this moisture condition at different confining pressures. The specimens were photographed before and after the mechanical testing.

The triaxial compression tests were carried out using radial strain as the feed back signal in order to obtain the complete response in the post-failure regime on brittle specimens as is described in the method description SKB MD 190.003, (SKB internal controlling document) and in the ISRM suggested method /1/. The axial ε_a and radial strain ε_r together with the axial stress σ_a were recorded during the test. The peak value of the axial compressive stress σ_c was determined at each test. Furthermore, two elasticity parameters, Young's modulus E and Poisson ratio v, were deduced from the tangent properties at 50% of the peak load. Diagrams with the volumetric and crack volumetric strain versus axial stress are reported. These diagrams can be used to determine crack initiation stress σ_i and the crack damage stress σ_d, cf. /2, 3/.

Figure 1-1. *Location of the borehole at the Oskarshamn site.*

2 Objective and scope

The purpose of the testing is to determine the compressive strength and the elastic properties, represented by the Young's modulus and the Poisson ratio, of confined cylindrical intact rock cores at different confining pressures. Moreover, the specimens have a water content corresponding to the in-situ conditions. The loading is carried out into the post-failure regime in order to study the mechanical behaviour of the rock after cracking and thereby be able to determine the brittleness and residual strength. The specimens are from the borehole KSH01A, which is a telescope borehole of SKB-kemi type with a bore depth of 1,000 m.

The results from the tests are going to be used in the site descriptive rock mechanics model, which will be established for the candidate area selected for site investigations at Simpevarp.

3 Equipment

A circular saw with a diamond blade was used to cut the specimens to their final lengths. The surfaces were then grinded after cutting in a grinding machine in order to achieve a high-quality surface for the axial loading that complies with the required tolerances. The measurements of the specimen dimensions were made with a sliding calliper. Furthermore, the tolerances were checked by means of a dial indicator and a stone face plate. The specimen preparation is carried out in accordance with ASTM 4543-01 /4/.

The specimens and the water were weighted using a scale for weight measurement. A thermometer was used for the water temperature measurement. The calculated wet density was determined with an uncertainty of ± 4 kg/m^3.

The mechanical tests were carried out in servo controlled testing machine specially designed for rock tests, see Figure 3-1. The system contains of a load frame, a hydraulic pump unit, a controller unit and various sensors. The communication with the controller unit is made by means of special testing software running on a PC that is connected to the controller. The load frame has a high stiffness and a fast responding actuator, cf. the ISRM suggested method /1/. Furthermore, the sensors, the controller and the servo valve are fast responding components. The machine is equipped with a pressure vessel in which the specimens are tested under a confinement pressure. A thin rubber membrane is mounted on the specimen in order to seal the specimen from the oil used that is used as the confinement medium, cf. Figure 3-2. The axial load is determined using a load cell, which is located inside the pressure vessel and has a maximum capacity of 1.5 MN. The uncertainty of the load measurement is less than 1%.

The axial and circumferential (radial) deformations of the rock specimen were measured. The rock deformation measurement systems are based on miniature LVDTs, which has a measurement range of +/– 2.5 mm. The LVDTs were calibrated by means of a micrometer and they displayed an accuracy of +/– 2.5% within a +/– 2 mm range that was used in the tests. The axial deformation measurement system comprises two aluminium rings that are attached on the specimen placed approximately at ¼ and ¾ of the specimen height, cf. Figures 3-2 and 4-1. Two LVDTs mounted on the rings are used to measure the distance change between the rings on opposite side of the specimen. The rings have three adjustable spring-loaded screws each with a rounded tip pointing towards the specimen with 120 degrees division. The rings are mounted directly on the rubber membrane. The pre-load of the screws fixates the rings. The position of the frame piston was also stored during the test in order to give a possibility for comparison with the measurements made with the measurement system that was based on the rings displacement.

The radial deformation was obtained by using a chain mounted around the specimen at mid-height, see Figure 3-2. The change of the chain-opening gap was measured by means of one LVDT and the circumferential and thereby also the radial deformation could be obtained. See Appendix A.

The specimens were photographed with a 4.0 Mega pixel digital camera at highest resolution and the photographs were stored in a jpeg-format.

Figure 3-1. *Left: Digital controller unit, pressure cabinet with cell pressure intensifier and oil reservoir inside, load frame with closed cell (pressure vessel). Right: Bottom of the cell is lowered. The specimen is instrumented and ready for inserting in the cell.*

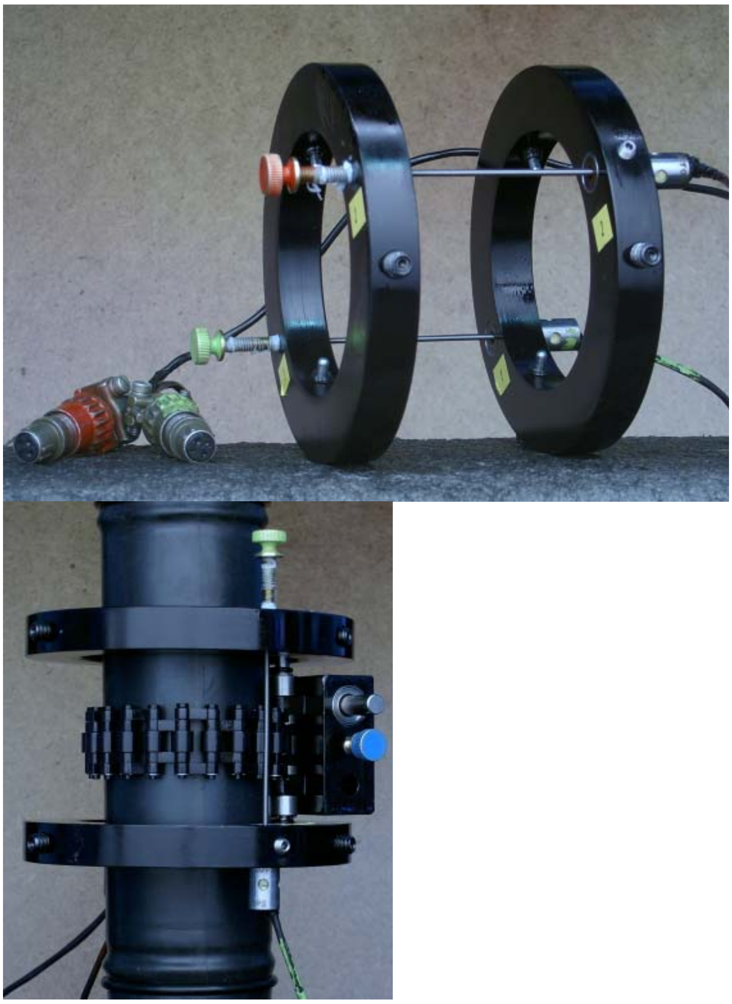

Figure 3-2. *Left: Rings and LVDTs for axial deformation measurement. Right: Specimen and loading platens sealed with a rubber membrane. Devices for axial and circumferential deformation measurements are attached.*

4 Execution

The water saturation and determination of the density of the wet specimens were made in accordance with the method description SKB MD 160.002, (SKB internal controlling document). This includes determination of density in accordance to ISRM /5/ and water saturation by SS EN 13755 /6/. The triaxial compression tests were carried out according to the method description SKB MD 190.003, (SKB internal controlling document). The test method is based on the ISRM suggested methods /1/ and /7/.

4.1 Description of the samples

The rock type characterisation was made according to Stråhle /8/ using the SKB mapping (Boremap). The identification marks, upper and lower sampling depth (Secup and Seclow) and the rock type are shown in Table 4-1.

Table 4-1. Specimen identification, sampling depth, confining pressure at the triaxial tests and rock type for all specimens.

Identification	Secup (m)	Seclow (m)	Confining pressure (MPa)	Rock type
KSH01A-115-1	298.81	298.86	2	Quartz monzodiorite
KSH01A-115-3	306.23	306.38	7	Quartz monzodiorite
KSH01A-115-5	312.86	313.01	2	Quartz monzodiorite
KSH01A-115-7	321.00	321.15	7	Quartz monzodiorite
KSH01A-115-9	321.58	321.73	10	Quartz monzodiorite
KSH01A-115-11	481.22	481.37	2	Fine-grained dioritoid
KSH01A-115-12	485.50	485.65	7	Fine-grained dioritoid
KSH01A-115-13	486.64	486.79	7	Fine-grained dioritoid
KSH01A-115-14	492.10	492.25	10	Fine-grained dioritoid
KSH01A-115-17	707.77	707.92	7	Quartz monzodiorite
KSH01A-115-18	709.24	709.39	7	Quartz monzodiorite
KSH01A-115-19	713.02	713.17	10	Quartz monzodiorite
KSH01A-115-20	713.70	713.85	2	Quartz monzodiorite

4.2 Testing

A step-by step description of the full test procedure is as follows:

Step	Activity
1	The drill cores were marked where the samples are to be taken.
2	The samples were cut to the specified length according to markings and the cutting surfaces were grinded.
3	The tolerances were checked: parallel and perpendicular end surfaces, smooth and straight circumferential surface.
4	The diameter and height were measured three times each. The respectively mean value determines the dimensions that are reported.
5	The samples were then water saturated according to the method described in SKB MD 160.002, (SKB internal controlling document) and were stored for minimum 7 days in water whereupon the wet density was determined.
6	Digital photos were then taken on each specimen before the mechanical testing.
7	The specimen was put in testing position and centred between the loading platens.
8	A rubber membrane was mounted on the specimen and the devices for measuring axial and circumferential deformations were attached to the specimen on top of the rubber membrane.
9	The core on each LVDT was adjusted by means of a set screw to the right initial position. This was done so that the optimal range of the LVDTs can be used for the deformation measurement.
10	The triaxial cell was closed and filled will oil whereby a cell pressure of 0.6 MPa is applied.
11	The frame piston was brought down into contact with the specimen with a force corresponding to a deviatoric stress of 0.6 MPa. The cell pressure was then raised to the specified level and at the same time keeping the deviatoric stress constant.
12	The deformation measurement channels were zeroed in the test software.
13	The loading was started and the initial loading rate was set to a radial strain rate of –0.025%/min. The loading rate was increased after reaching the post-failure region. This was done in order to prevent the total time for the test to become too long.
14	The test was stopped either manually when the test had proceeded large enough to see the post-failure behaviour, or after severe cracking had occurred and it was judged that very little residual axial loading capacity was left in the specimen.
15	The oil pressure was brought down to zero and the oil was poured out of the cell. The cell was opened and the specimen is taken out.
16	Digital photos were taken on each sample after the mechanical testing.

The temperature of the water was 18.4°C, which equals to a water density of 998.5 kg/m^3, when the determination of density of the rock specimens was carried out. Further, the specimens had been stored 10 days in water when the density was determined and 24–27 days when the triaxial compression tests were carried out. The functionality of the system was checked, by carrying out tests on other cores with a similar type rock before the tests described in this report started. A check-list was filled in successively during the work in order to confirm that the different specified steps have been carried out. Moreover, comments were made upon observed things during the mechanical testing that are relevant for the interpretation of the results. The check-list form is a SP internal quality document.

4.3 Data handling

The test results were exported as text files from the test software and stored in a file server on the SP computer network after each completed test. The main data processing, in which the elastic moduli were computed and the peak stress was determined, has been carried out in the program MATLAB /9/. Moreover, MATLAB was used to produce the diagrams shown in Section 5.1 and in Appendix B. The summary of results in Section 5.2 with tables containing mean value and standard deviation of the different parameters and diagrams were produced using MS Excel. MS Excel was also used for reporting data to the SICADA database.

4.4 Analyses and interpretation

As to the definition of the different results parameters we begin with the axial stress σ_a, which is defined as

$$\sigma_a = \frac{F}{A}$$

where F is the axial force acting on the specimen and A is specimen cross section area. The pressure vessel (triaxial cell) filled with oil specimen is pressurized with a cell (confining) pressure p_c. This implies that the specimen becomes confined and the radial stress σ_r of the specimen is equal to confining pressure p. The (effective) deviatoric stress is defined as

$$\sigma_{dev} = \sigma_a - \sigma_r$$

The peak value of the axial stress during a test is representing the triaxial compressive strength σ_c, for the actual confining pressure used in the test, in the results presentation.

The average value of the two axial displacement measurements on opposite sides of the specimen is used for the axial strain calculation. The recorded deformation δ_{local} represents a local axial displacement between the points approximately at ¼ and ¾ of the specimen height, cf. Figure 4-1. The axial strain is defined as

$$\varepsilon_a = \delta_{local}/L_{local}$$

where L_{local} is the distance between the rings before loading.

The radial deformation is measured by means of a chain mounted around the specimen at mid-height, see Figure 3-2. The change of chain opening gap is measured by means of one LVDT. This measurement is used to compute the radial strain ε_r, see Appendix A. Moreover, the volumetric strain ε_{vol} is defined as

$$\varepsilon_{vol} = \varepsilon_a + 2\varepsilon_r$$

The stresses and the strains are defined as positive in compressive loading and deformation. The elasticity parameters are defined by the tangent Young's modulus E and tangent Poisson ratio v as

$$E = \frac{\sigma_a(0.55\sigma_c) - \sigma_a(0.45\sigma_c)}{\varepsilon_a(0.55\sigma_c) - \varepsilon_a(0.45\sigma_c)}$$

$$\nu = -\frac{\varepsilon_r(0.55\sigma_c) - \varepsilon_r(0.45\sigma_c)}{\varepsilon_a(0.55\sigma_c) - \varepsilon_a(0.45\sigma_c)}$$

The tangents were evaluated with values corresponding to an axial load between 45% and 55% of the axial peak stress σ_c.

A closure of present micro cracks will take place initially during confinement and axial loading. Development of new micro cracks will start when the axial load is further increased and axial stress reaches the crack initiation stress σ_i. The crack growth at this stage is as stable as increased loading is required for further cracking. A transition from a development of micro cracks to macro cracks will take place when the axial load is further increased. At a certain stress level the crack growth becomes unstable. The stress level when this happens is denoted the crack damage stress σ_d, cf. /2, 3/. In order to determine the stress levels we look at the volumetric strain.

By subtracting the elastic volumetric strain ε_{vol}^{e} from the total volumetric strain a volumetric strain corresponding to the crack volume is obtained ε_{vol}^{cr}. This has been denoted calculated crack volumetric strain in the literature, cf. /2, 3/. We have thus

$$\varepsilon_{vol}^{cr} = \varepsilon_{vol} - \varepsilon_{vol}^{e}$$

Assuming linear elasticity leads to

$$\varepsilon_{vol}^{cr} = \varepsilon_{vol} - \frac{1-2\nu}{E}(\sigma_a - \sigma_r)$$

Experimental investigations have shown that the crack initiation stress σ_i coincides with the onset of increase of the calculated crack volume, cf. /2, 3/. The same investigations also indicate that the crack damage stress σ_d can be defined as the axial stress at which the total volume starts to increase, i.e. when a dilatant behaviour is observed.

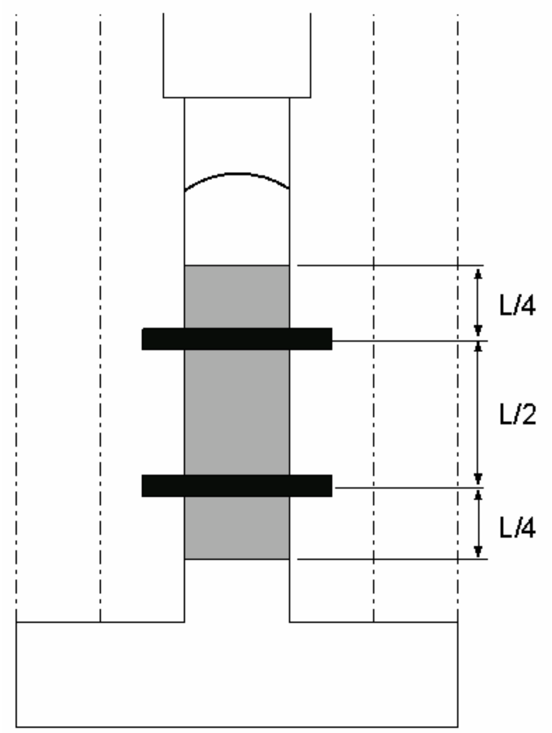

Figure 4-1. *Sketch showing the triaxial cell with the rock specimen (grey) with height L and the placement of the rings (black) used for the axial deformation measurements. The membrane is omitted in the figure for simplicity.*

5 Results

The results of the individual specimens are presented in Section 5.1 and a summary of the results is given in Section 5.2. The reported parameters are based on unprocessed raw data obtained from the testing and were reported to the SICADA database, FN 96. These data together with the digital photographs of the individual specimens were stored on a CD and handed over to SKB. The handling of the results follows SDP-508 (SKB internal controlling document) in general.

5.1 Description and presentation of the specimen

The cracking is shown in pictures taken on the specimens with comments on observed things that appeared during the testing. The elasticity parameters have been evaluated by using the results from the local deformation measurements. Red rings are superposed on the graphs indicating every five minutes of the progress of testing. The results for the individual specimens are as follows:

Specimen ID: KSH01A-115-1

Before mechanical test

After mechanical test

Diameter (mm)	**Height (mm)**	**Density (kg/m^3)**
50.1	126.4	2,770

Comments

Specimen ID: KSH01A−115−01

Youngs Modulus (E):	67.8	[GPa]	Cell pressure:	2	[MPa]
Poisson Ratio (ν):	0.226	[−]			
Axial peak stress (σ_c):	181.6	[MPa]			

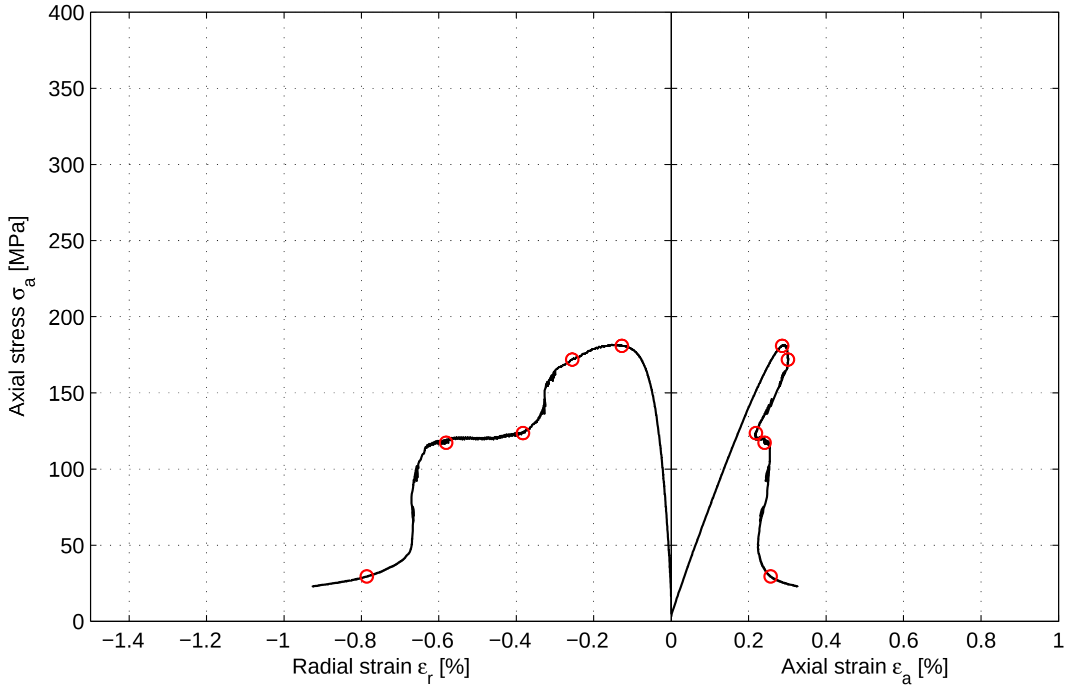

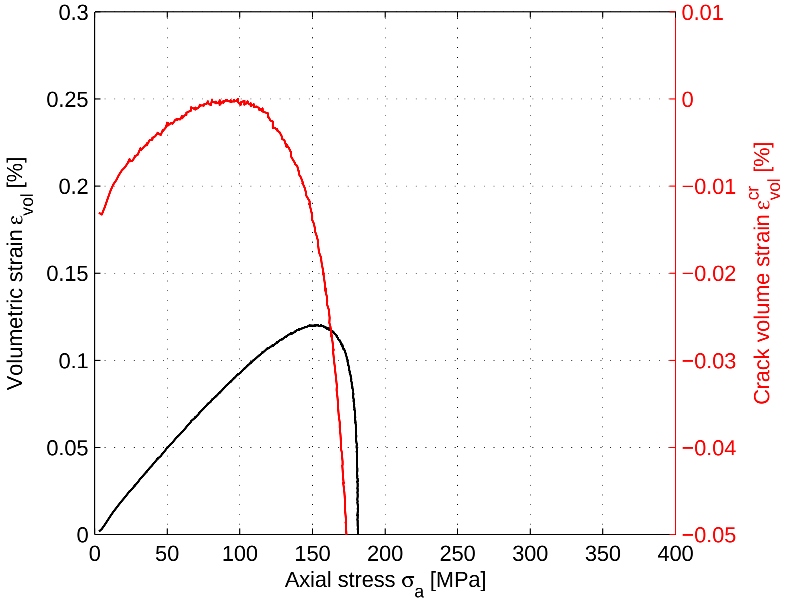

Specimen ID: KSH01A-115-3

Before mechanical test

After mechanical test

Diameter (mm)	**Height (mm)**	**Density (kg/m^3)**
50.2	126.4	2,790

Comments The membrane had a small leakage.

Specimen ID: KSH01A−115−03

Youngs Modulus (E):	89.1	[GPa]	Cell pressure:	7	[MPa]
Poisson Ratio (ν):	0.22	[−]			
Axial peak stress (σ_c):	245.8	[MPa]			

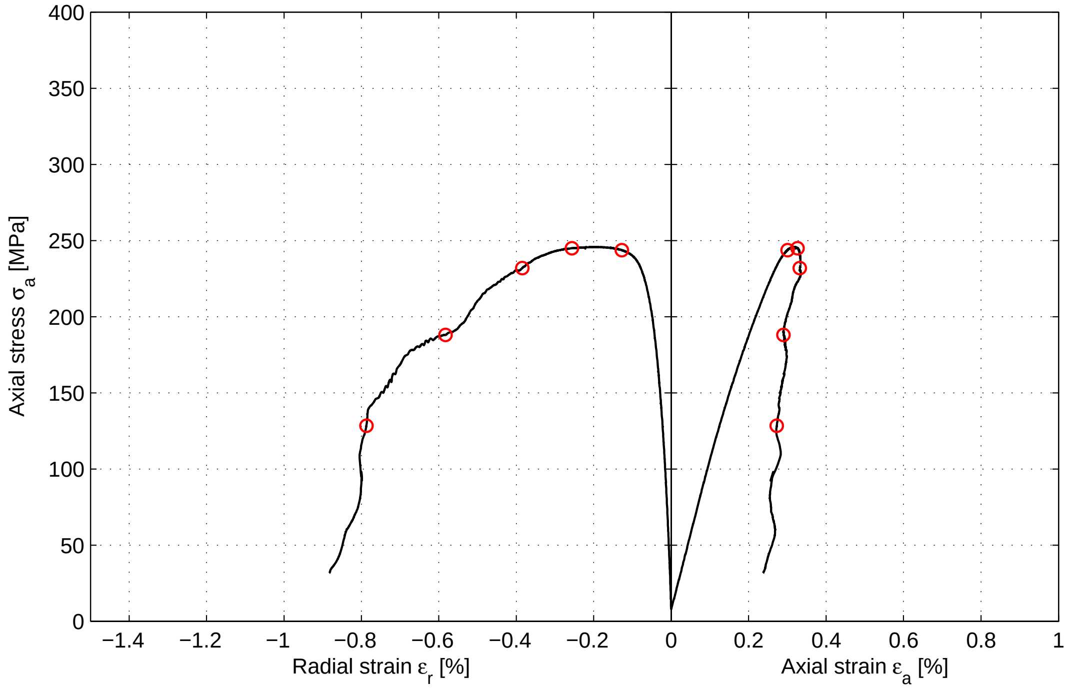

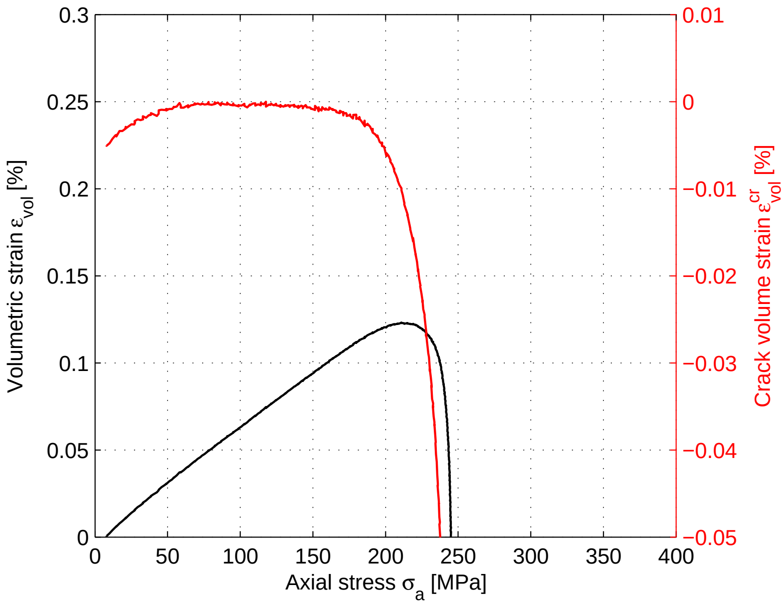

Specimen ID: KSH01A-115-5

Before mechanical test

After mechanical test

Diameter (mm)	**Height (mm)**	**Density (kg/m^3)**
50.1	126.3	2,790

Comments

Specimen ID: KSH01A−115−05

Youngs Modulus (E):	67.6	[GPa]	Cell pressure:	2	[MPa]
Poisson Ratio (ν):	0.238	[−]			
Axial peak stress (σ_c):	194.2	[MPa]			

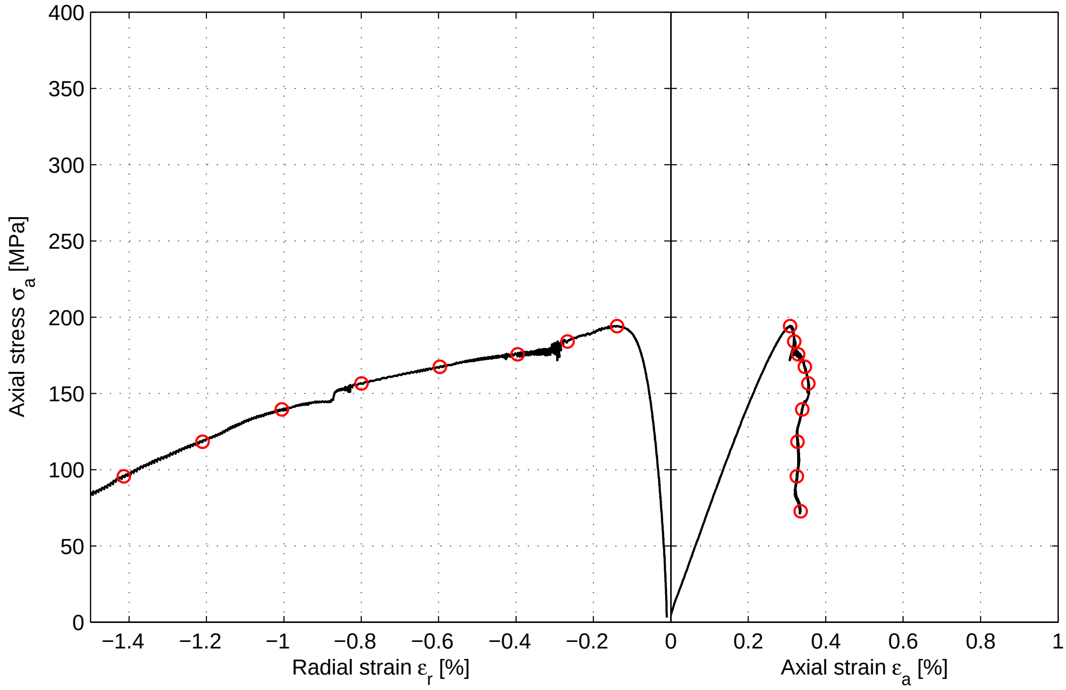

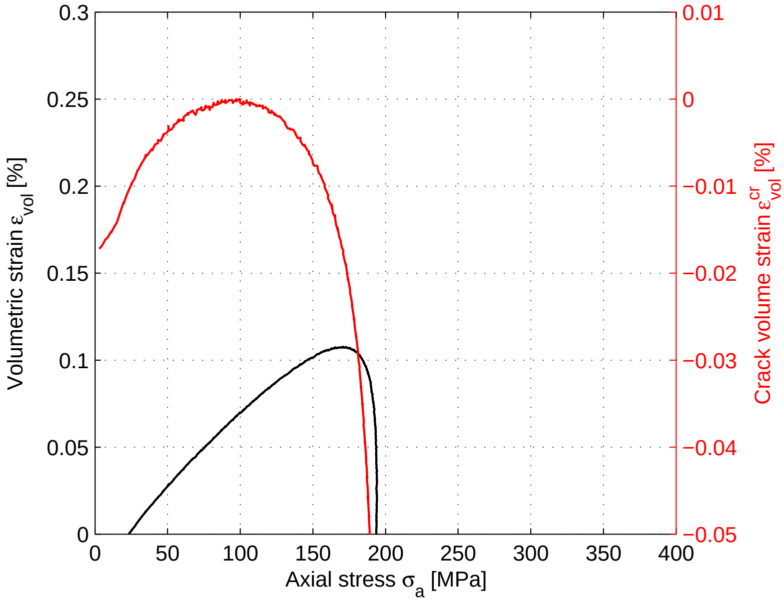

Specimen ID: KSH01A-115-7

Before mechanical test

After mechanical test

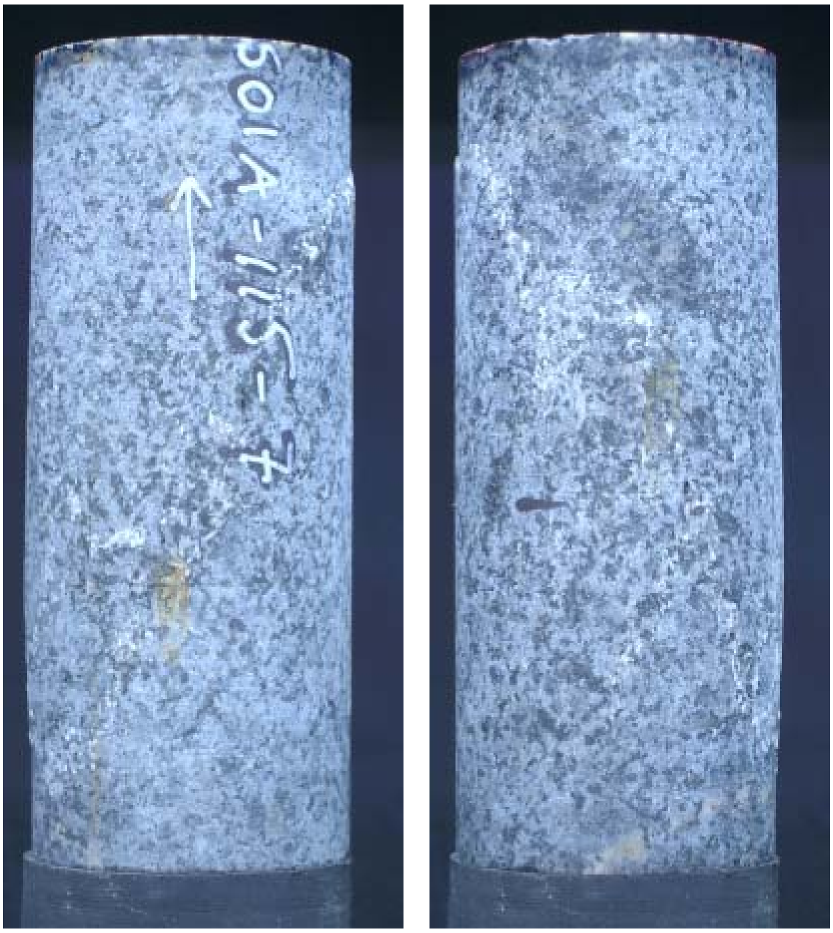

Diameter (mm)	**Height (mm)**	**Density (kg/m^3)**
50.1	126.3	2,810

Comments

Specimen ID: KSH01A−115−07

Youngs Modulus (E):	75.8	[GPa]	Cell pressure:	7	[MPa]
Poisson Ratio (ν):	0.223	[−]			
Axial peak stress (σ_c):	250.8	[MPa]			

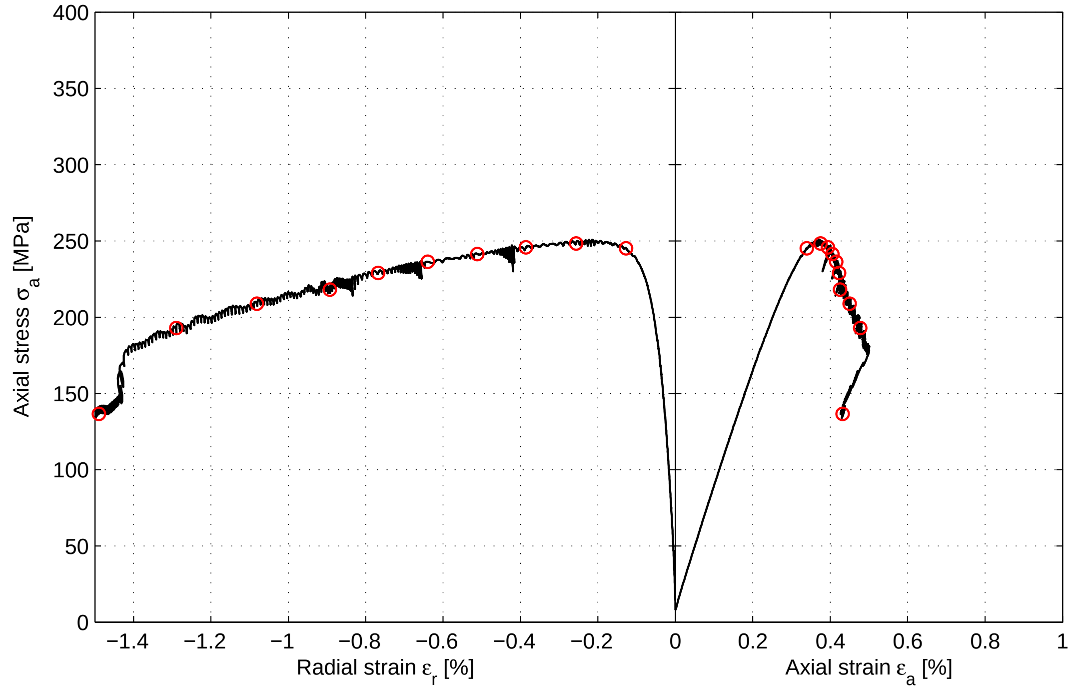

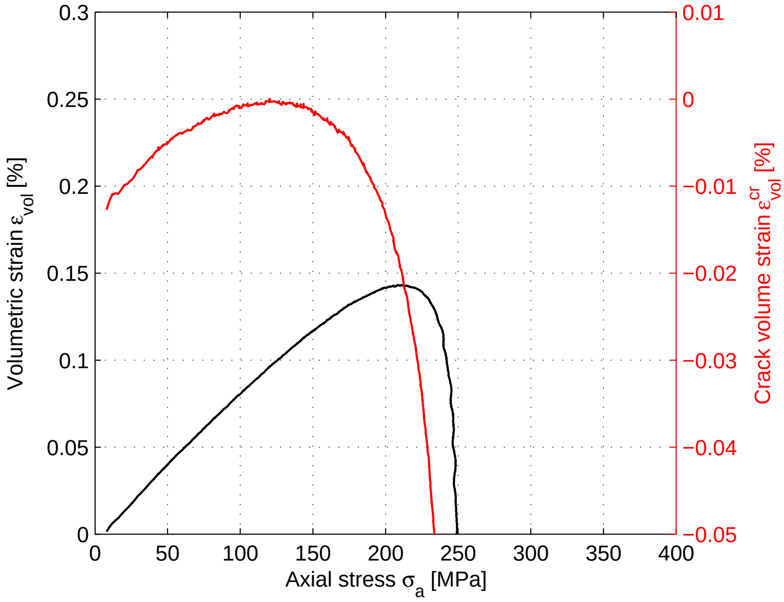

Specimen ID: KSH01A-115-9

Before mechanical test After mechanical test

Diameter (mm)	**Height (mm)**	**Density (kg/m^3)**
50.1	126.3	2,820

Comments

Specimen ID: KSH01A−115−09

Youngs Modulus (E):	79	[GPa]	Cell pressure:	10	[MPa]
Poisson Ratio (ν):	0.173	[−]			
Axial peak stress (σ_c):	289.6	[MPa]			

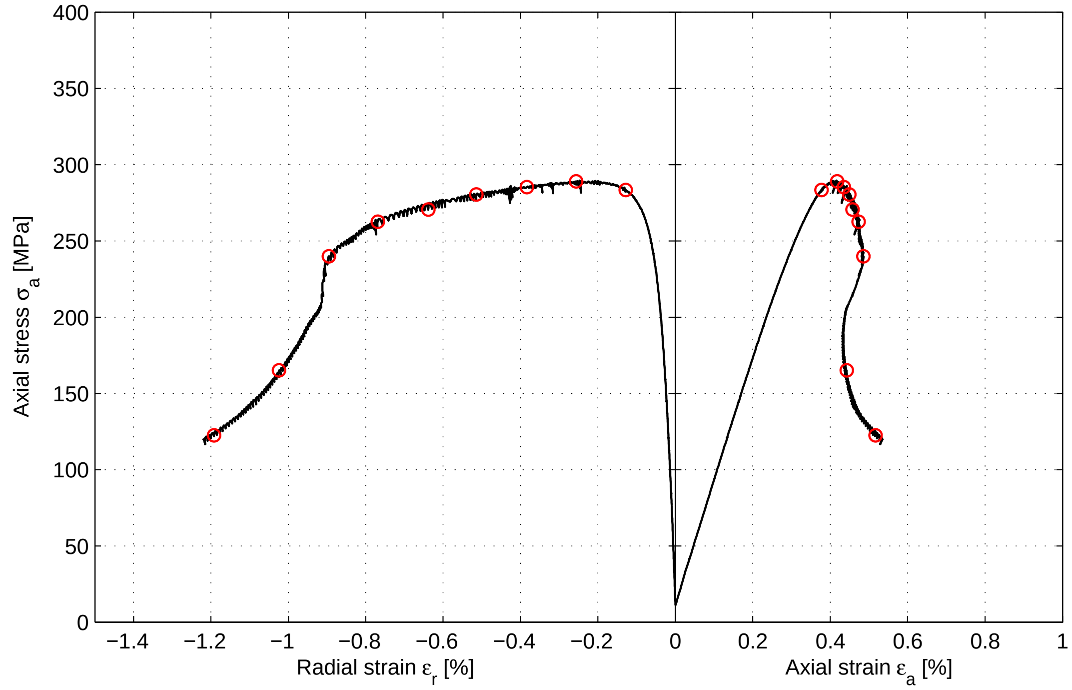

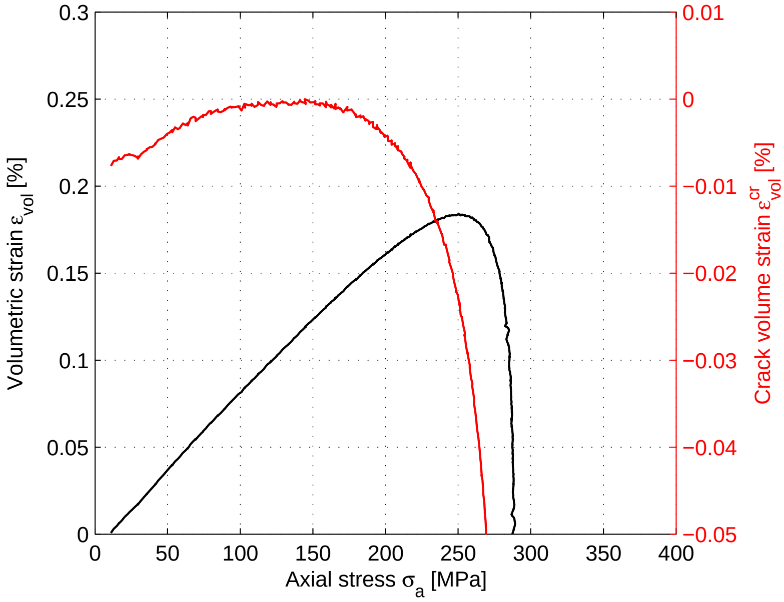

Specimen ID: KSH01A-115-11

Before mechanical test

After mechanical test

Diameter (mm)	Height (mm)	Density (kg/m^3)
50.1	126.9	2,780

Comments Cracking was initiated at an early stage in a pre-existent cured crack and a low peak stress was obtained.

Specimen ID: KSH01A−115−11

Youngs Modulus (E):	69.7	[GPa]	Cell pressure:	2	[MPa]
Poisson Ratio (ν):	0.153	[−]			
Axial peak stress (σ_c):	93.9	[MPa]			

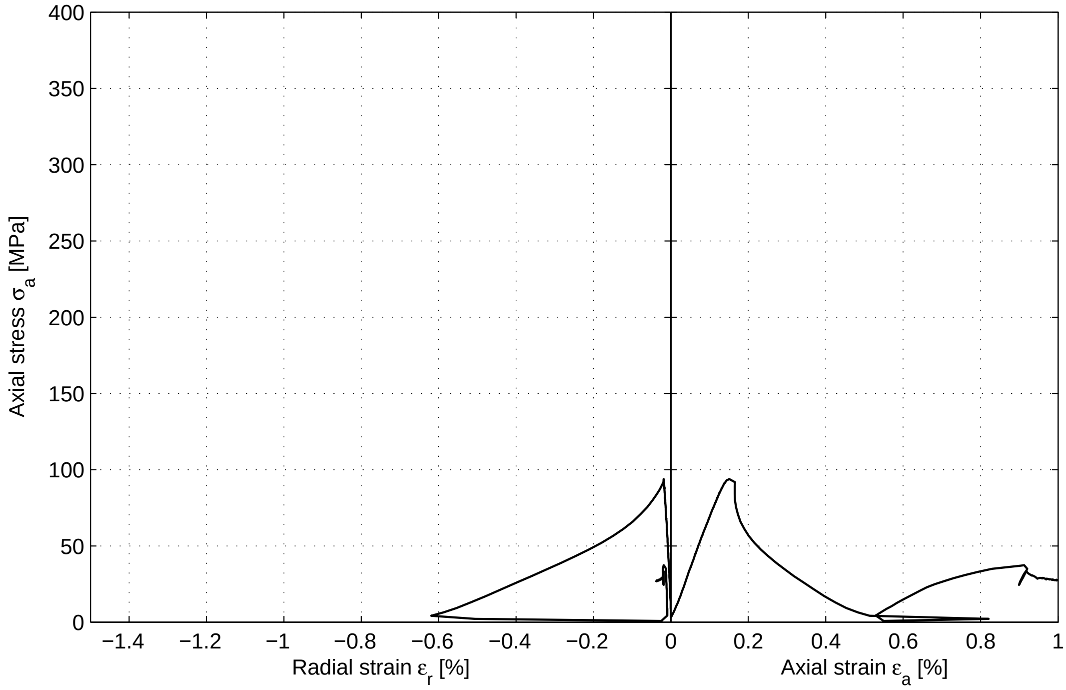

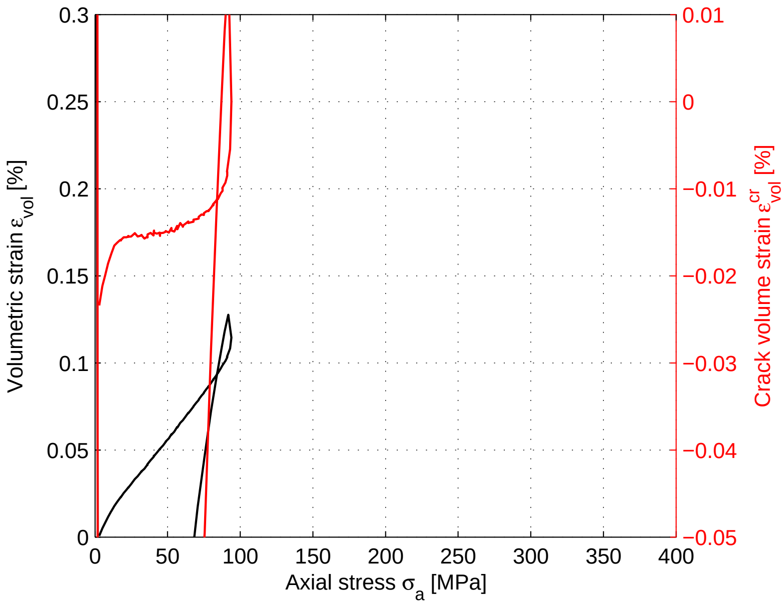

Specimen ID: KSH01A-115-12

Before mechanical test

After mechanical test

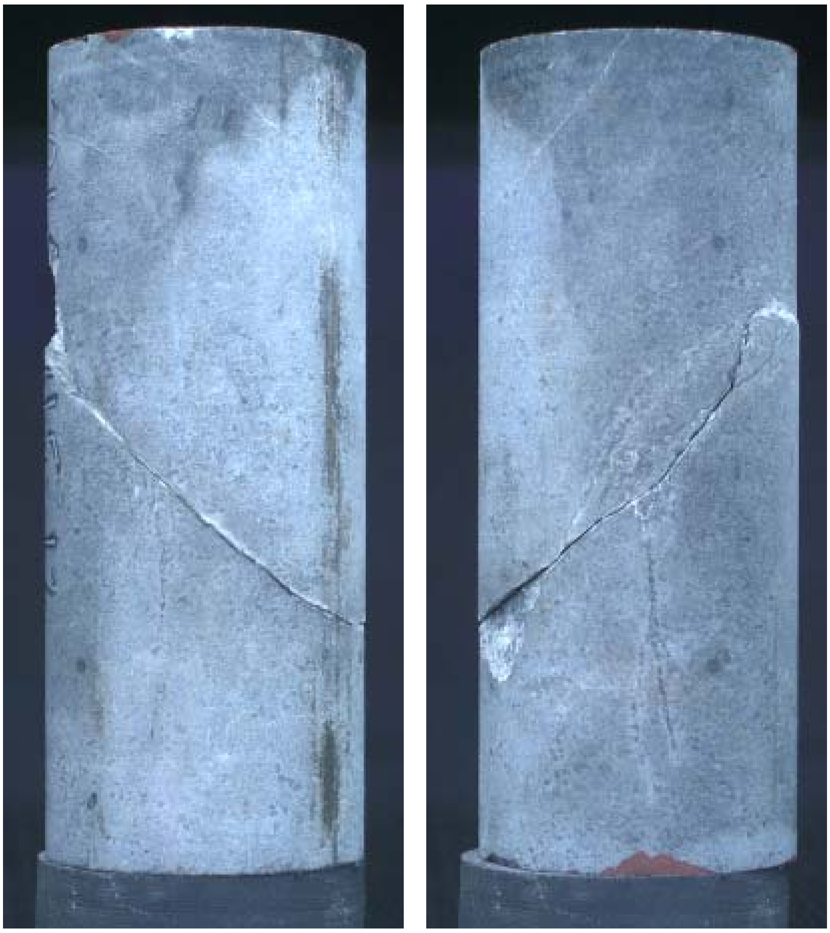

Diameter (mm)	**Height (mm)**	**Density (kg/m^3)**
50.1	126.9	2,800

Comments

Specimen ID: KSH01A−115−12

Youngs Modulus (E):	67.1	[GPa]	Cell pressure:	7	[MPa]
Poisson Ratio (ν):	0.22	[−]			
Axial peak stress (σ_c):	218	[MPa]			

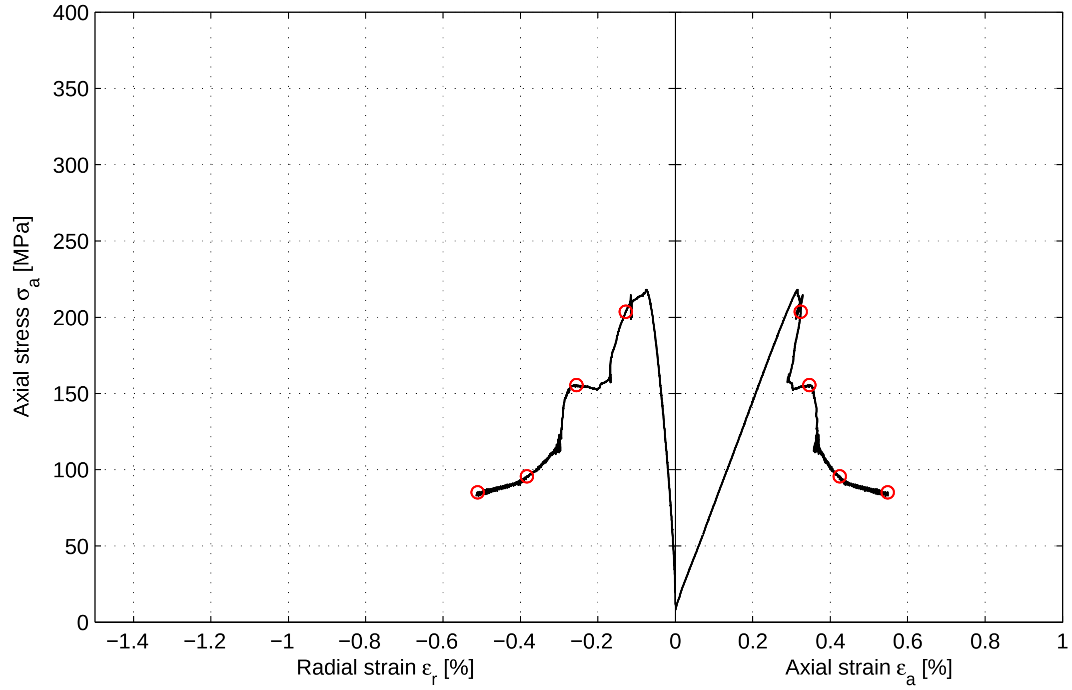

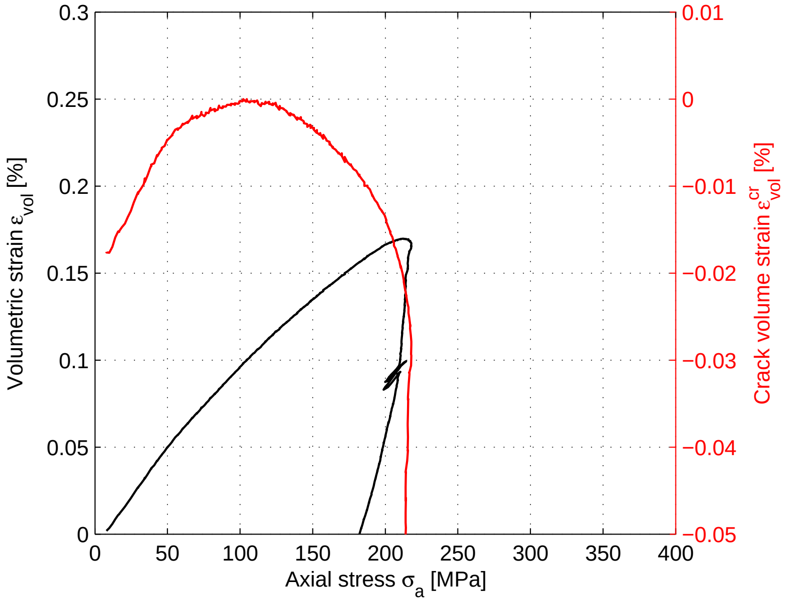

Specimen ID: KSH01A-115-13

Before mechanical test

After mechanical test

Diameter (mm)	**Height (mm)**	**Density (kg/m^3)**
50.1	126.9	2,800

Comments The membrane was punctured caused by pieces of the fractured rock.

Specimen ID: KSH01A−115−13

Youngs Modulus (E):	81.1	[GPa]	Cell pressure:	7	[MPa]
Poisson Ratio (ν):	0.209	[−]			
Axial peak stress (σ_c):	286.9	[MPa]			

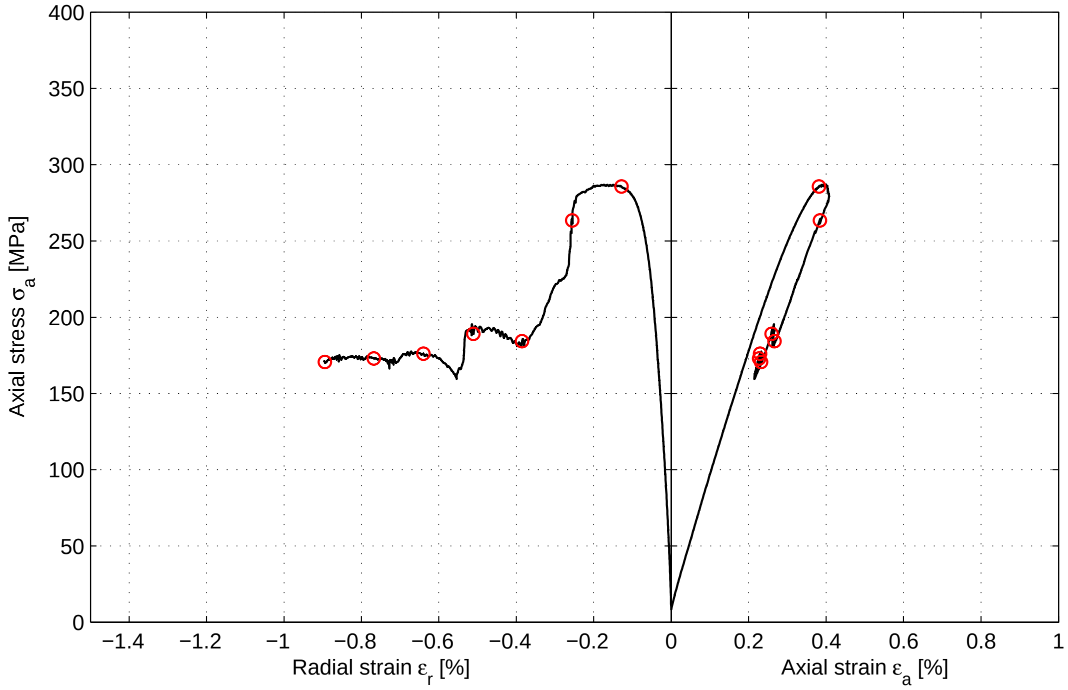

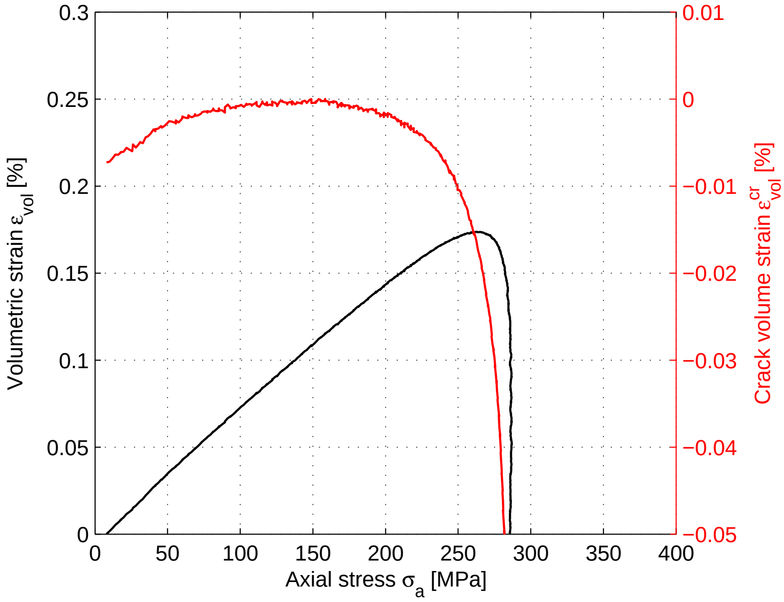

Specimen ID: KSH01A-115-14

Before mechanical test

After mechanical test

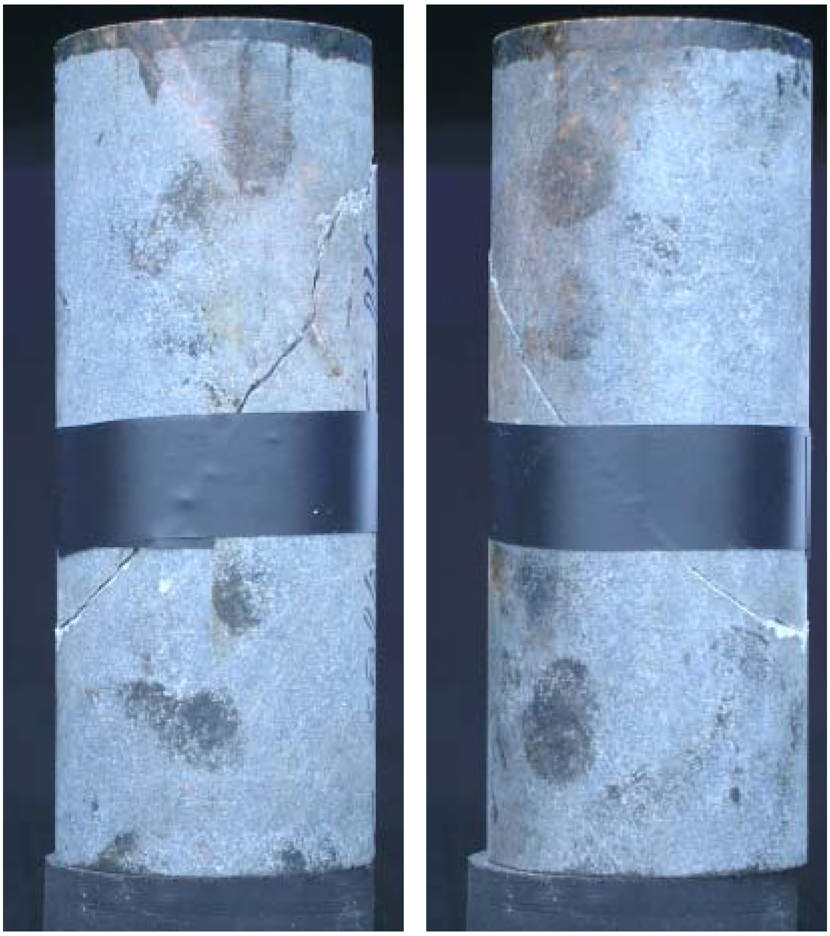

Diameter (mm)	**Height (mm)**	**Density (kg/m^3)**
50.1	127	2,790

Comments A sudden large increase of the radial deformation occurred due to cracking. The loading piston was then fully retracted. A shear failure was observed. The membrane had a small leakage.

Specimen ID: KSH01A−115−14

Youngs Modulus (E):	76.8	[GPa]	Cell pressure:	10	[MPa]
Poisson Ratio (ν):	0.235	[−]			
Axial peak stress (σ_c):	243.4	[MPa]			

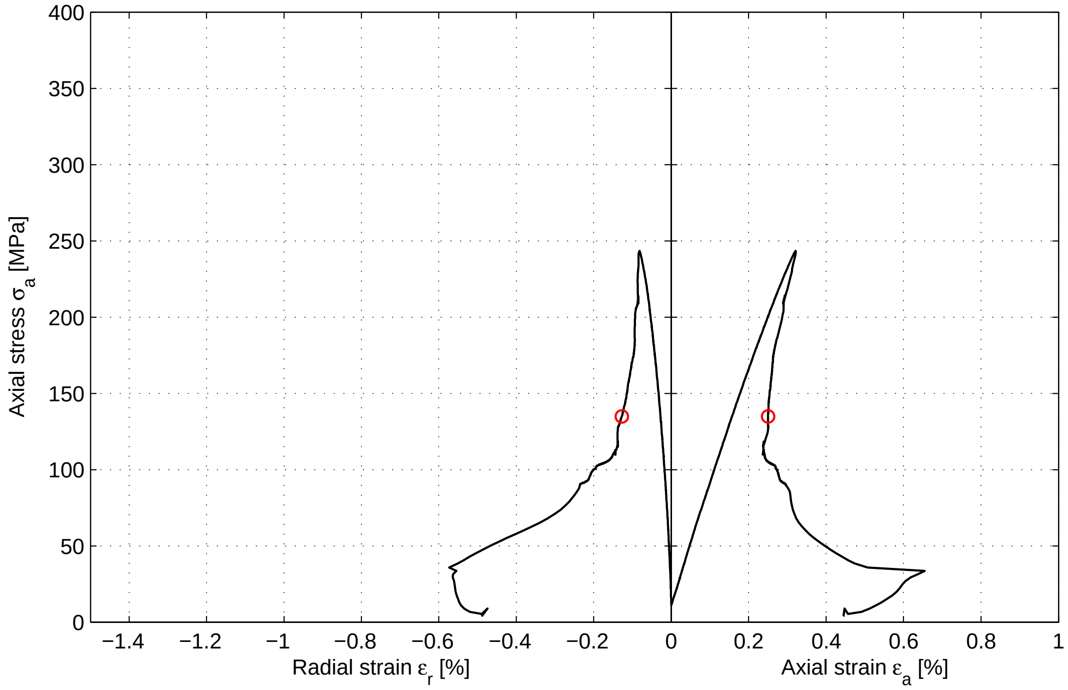

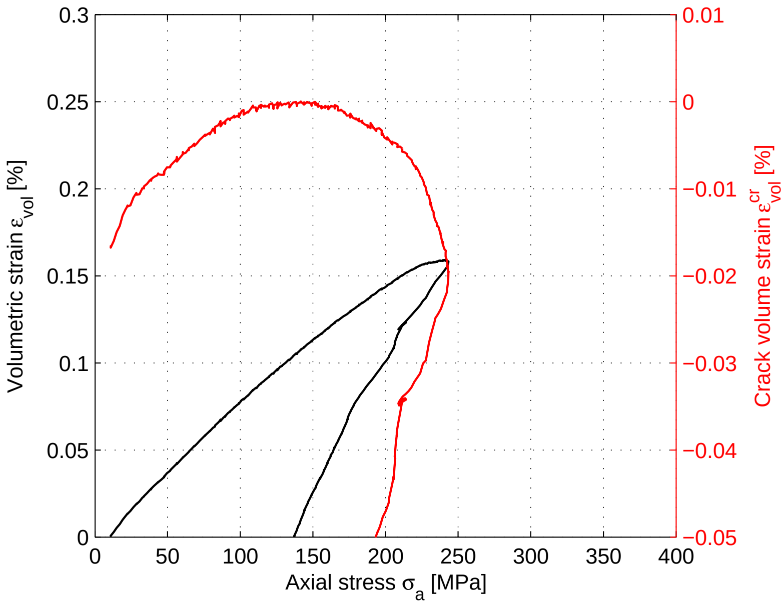

Specimen ID: KSH01A-115-17

Before mechanical test

After mechanical test

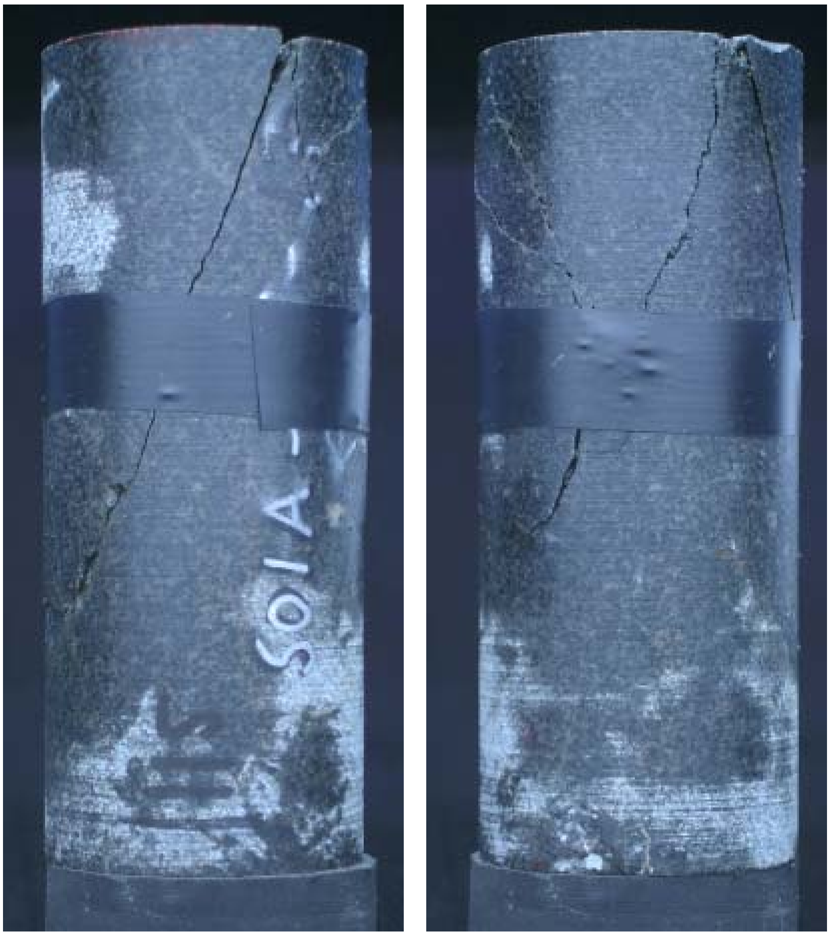

Diameter (mm)	**Height (mm)**	**Density (kg/m^3)**
50.1	126.9	2,870

Comments A sudden large increase of the radial deformation occurred due to cracking. The loading piston was then fully retracted. A shear failure was observed and the rubber membrane was punctured by the rock.

Specimen ID: KSH01A−115−17

Youngs Modulus (E):	73.8	[GPa]	Cell pressure:	7	[MPa]
Poisson Ratio (ν):	0.178	[−]			
Axial peak stress (σ_c):	199.2	[MPa]			

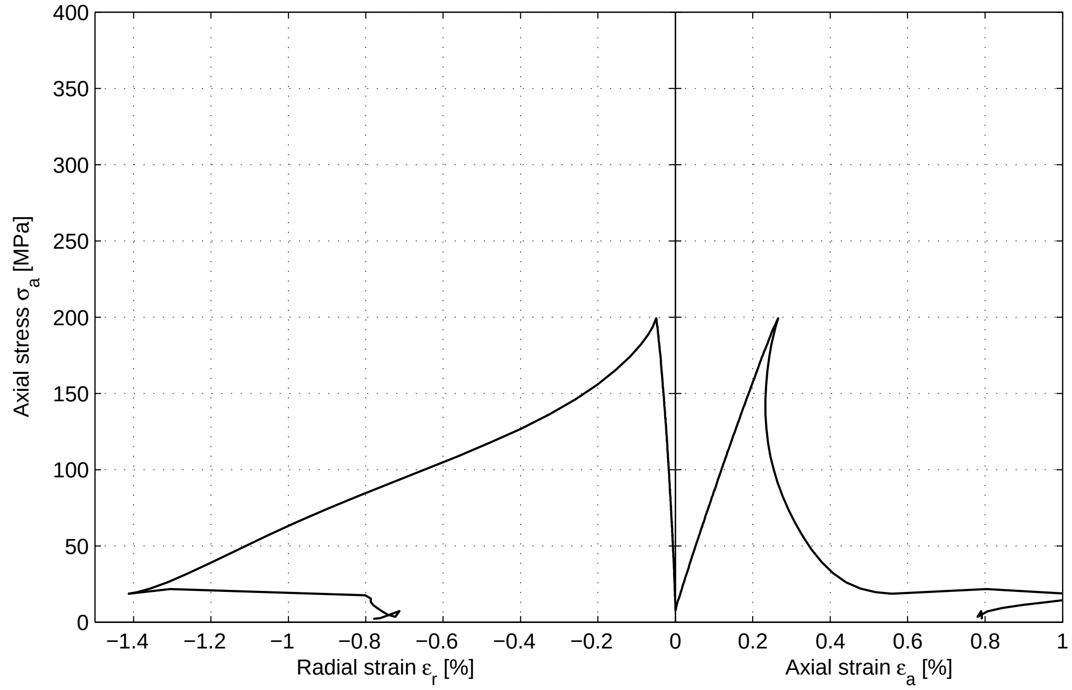

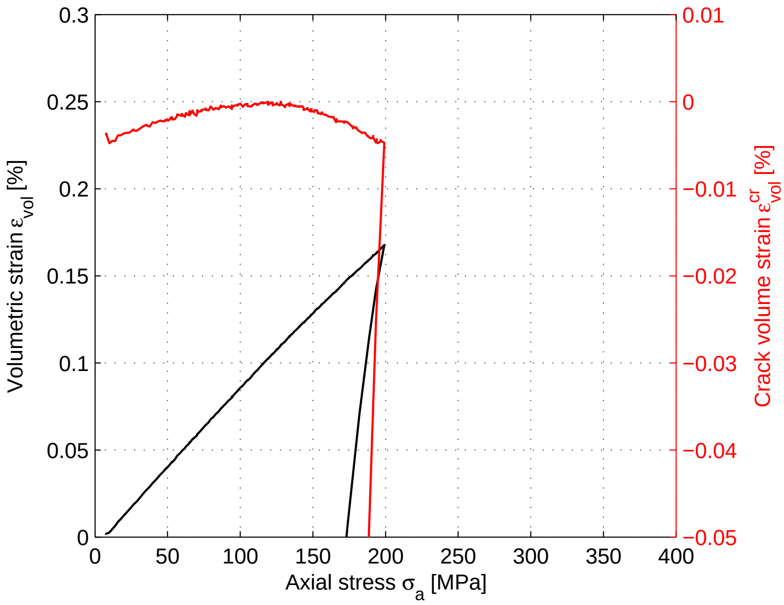

Specimen ID: KSH01A-115-18

Before mechanical test | After mechanical test

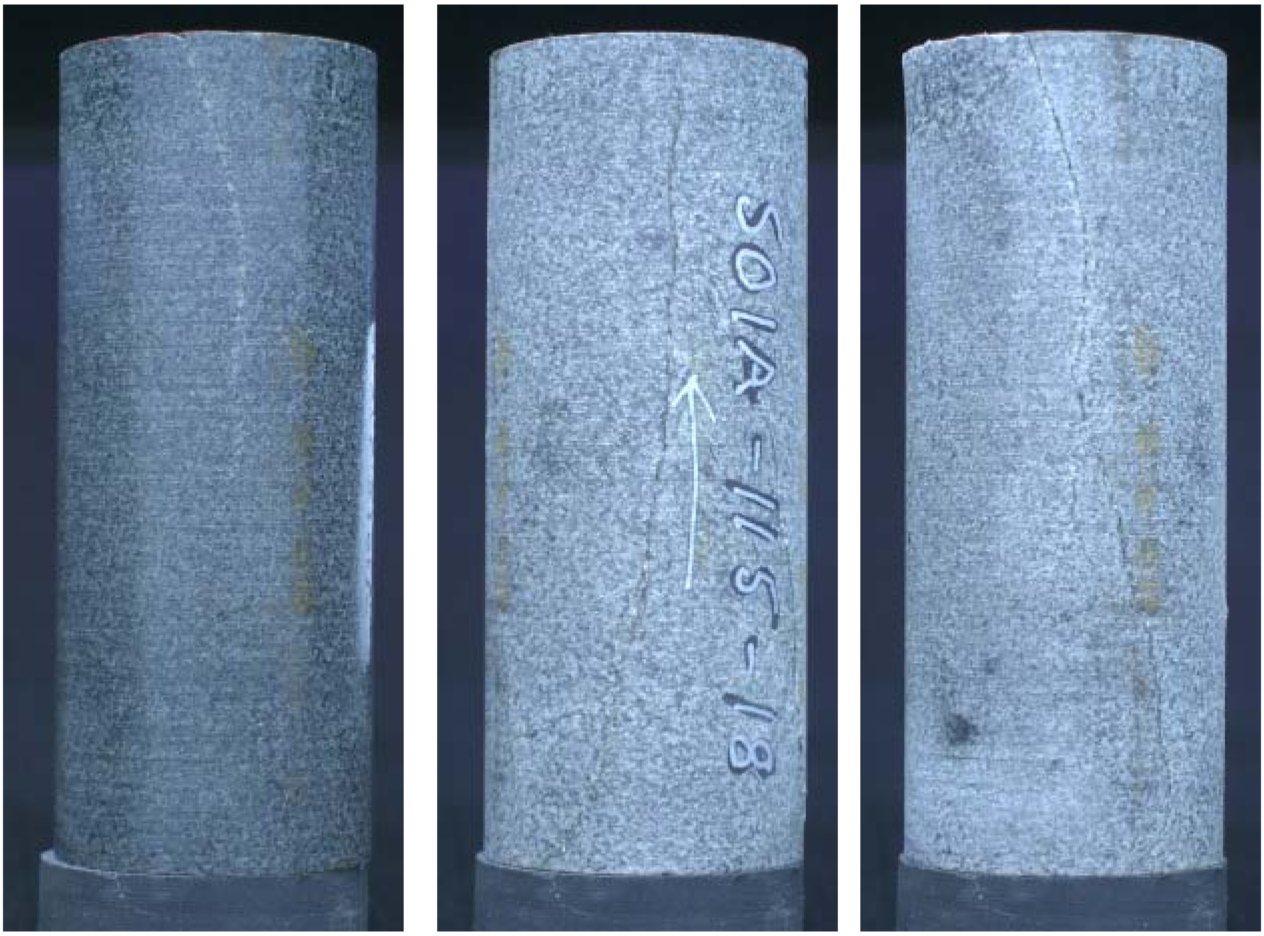

Diameter (mm)	**Height (mm)**	**Density (kg/m³)**
50.1	126.3	2,870

Comments

Specimen ID: KSH01A−115−18

Youngs Modulus (E):	72.9	[GPa]	Cell pressure:	7	[MPa]
Poisson Ratio (ν):	0.191	[−]			
Axial peak stress (σ_c):	256.5	[MPa]			

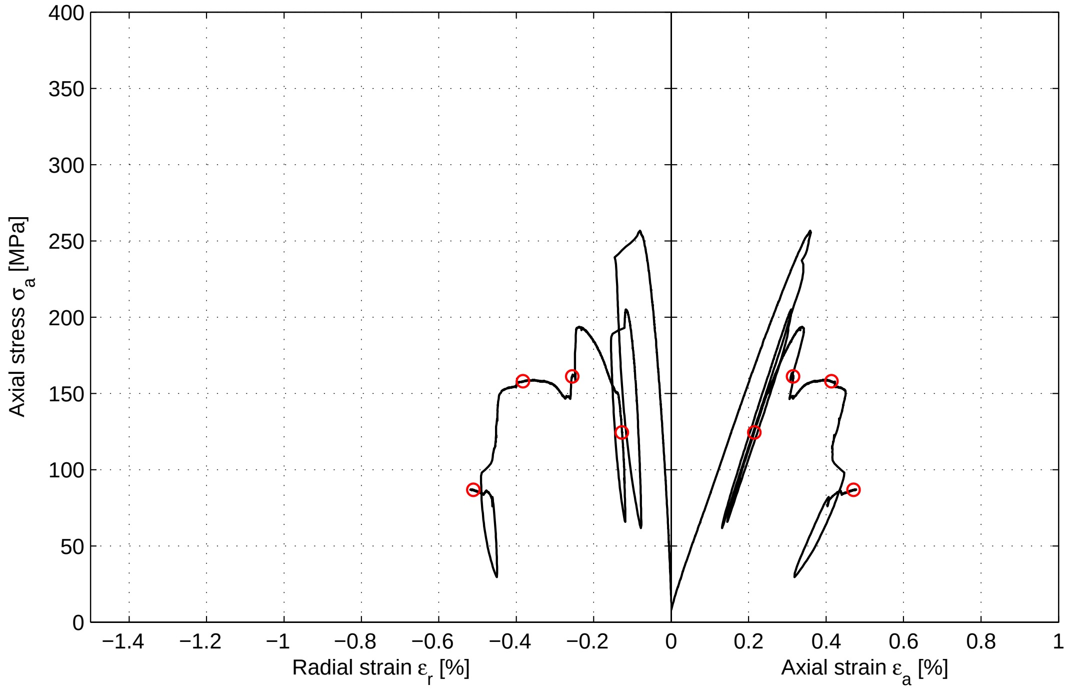

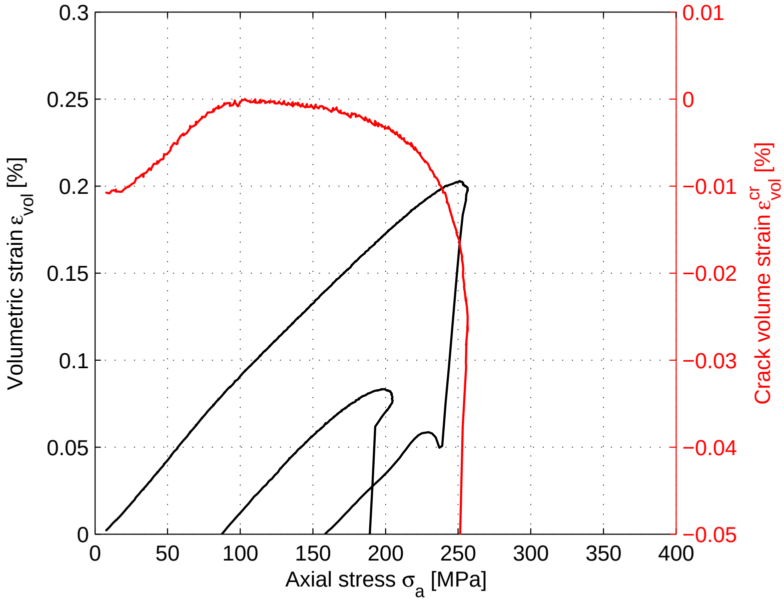

Specimen ID: KSH01A-115-19

Before mechanical test

After mechanical test

Diameter (mm)	**Height (mm)**	**Density (kg/m^3)**
50.1	126.2	2,870

Comments The membrane had a small leakage.

Specimen ID: KSH01A−115−19

Youngs Modulus (E):	89.2	[GPa]	Cell pressure:	10	[MPa]
Poisson Ratio (ν):	0.239	[−]			
Axial peak stress (σ_c):	216.2	[MPa]			

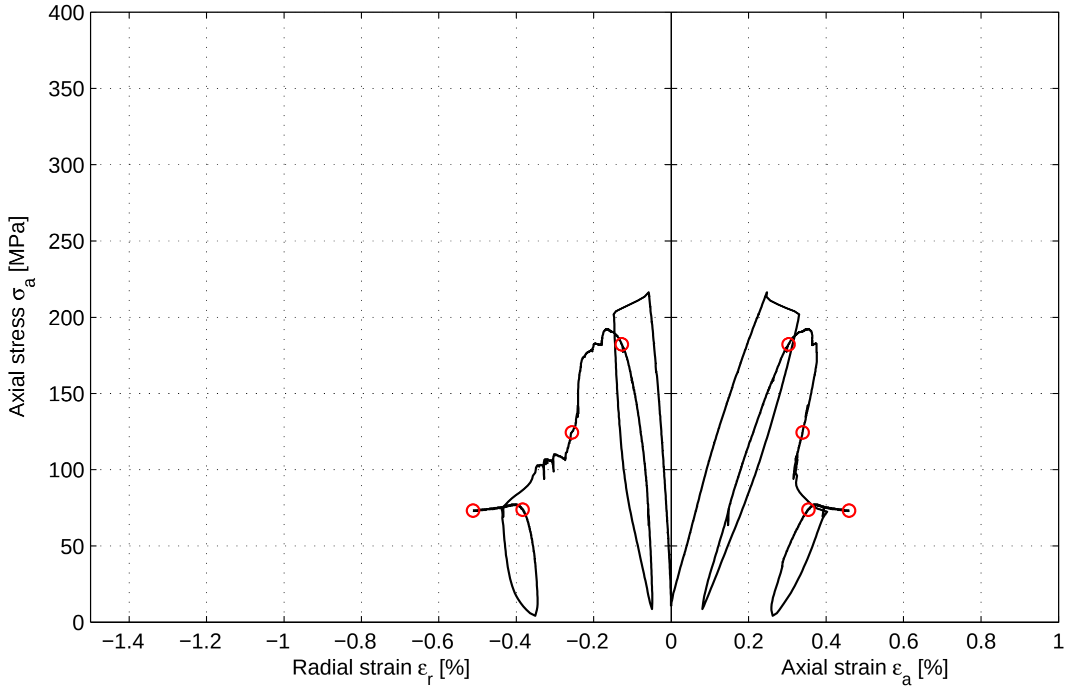

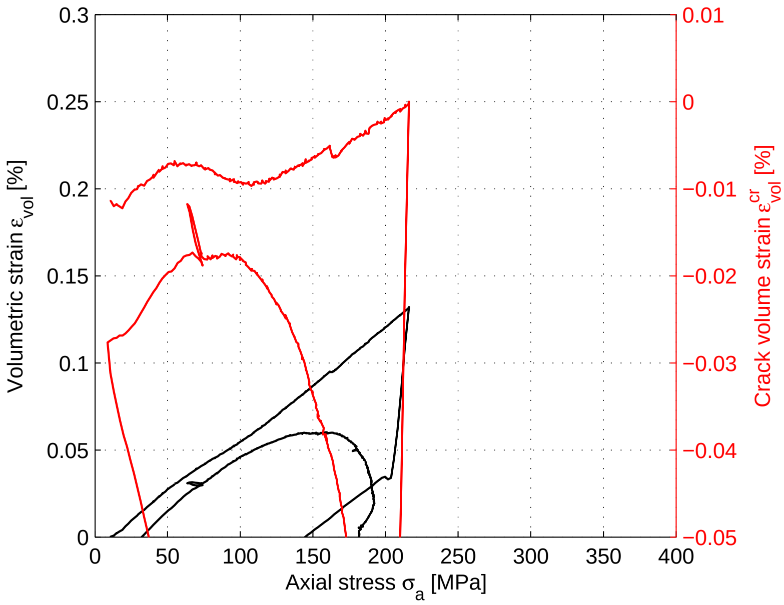

Specimen ID: KSH01A-115-20

Before mechanical test

After mechanical test

Diameter (mm)	Height (mm)	Density (kg/m^3)
50.1	126.4	2,860

Comments The test was restarted after a large sudden increase of the radial strain had occurred causing a complete unloading. The specimen had, however, very small residual strength left and the test was stopped.

Specimen ID: KSH01A−115−20

Youngs Modulus (E):	81.2	[GPa]	Cell pressure:	2	[MPa]
Poisson Ratio (ν):	0.19	[−]			
Axial peak stress (σ_c):	202.9	[MPa]			

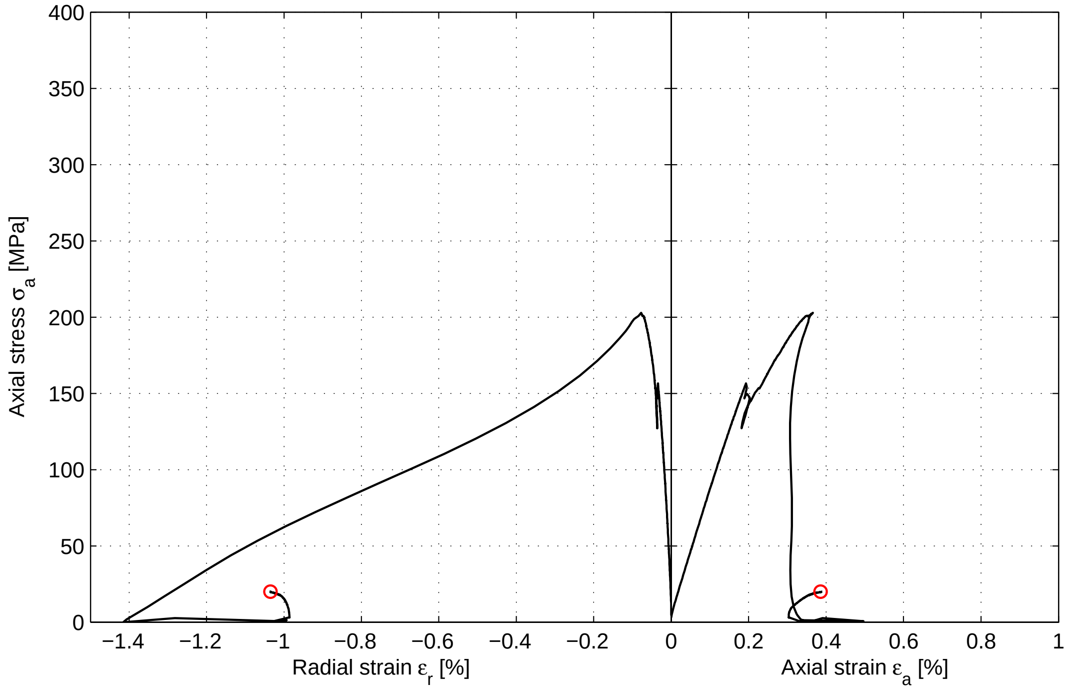

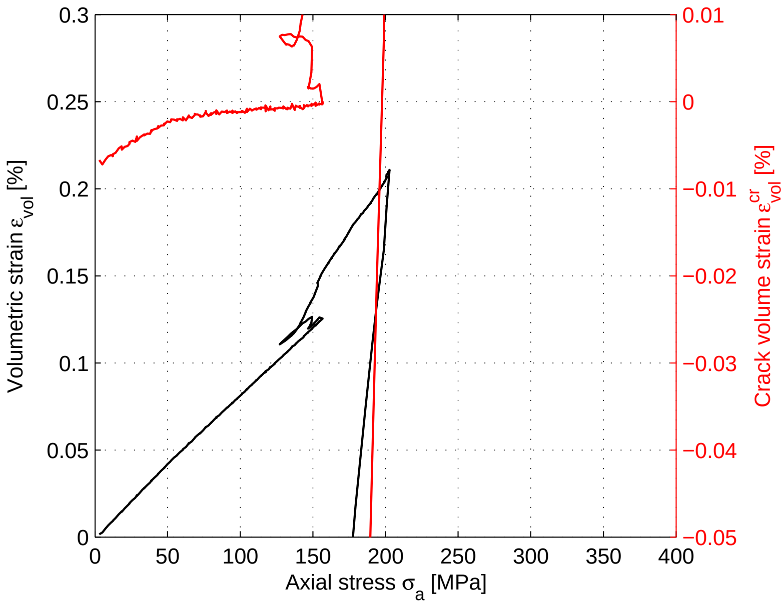

5.2 Results for the entire test series

A summary of the test results is shown in Tables 5-1 and 5-2. SKB has reviewed all results and excluded data that are not representative for the homogenous rock material, cf. Table 5-1. The densities, triaxial compressive strength, the tangent Young's modulus and the tangent Poisson ratio versus the depth, at which the samples are taken, are shown in Figures 5-1 to 5-4.

Table 5-1. Summary of results. The results in parenthesises denote results that are not representative for the homogenous rock material as defects in the specimens were observed.

Identification	Conf press (MPa)	Density (kg/m^3)	Compressive Strength (MPa)	Young's modulus (GPa)	Poisson ratio (–)	Comments
KSH01A-115-1	2	2,770	181.6	67.8	0.23	
KSH01A-115-3	7	2,790	245.8	89.1	0.22	
KSH01A-115-5	2	2,790	194.2	67.6	0.24	
KSH01A-115-7	7	2,810	250.8	75.8	0.22	
KSH01A-115-9	10	2,820	289.6	79.0	0.17	
KSH01A-115-11	2	2,780	(93.9)	(69.7)	(0.15)	Failure in weak zone
KSH01A-115-12	7	2,800	218.0	67.1	0.22	
KSH01A-115-13	7	2,800	286.9	81.1	0.21	
KSH01A-115-14	10	2,790	243.4	76.8	0.24	
KSH01A-115-17	7	2,870	(199.2)	73.8	0.18	Unfinished test
KSH01A-115-18	7	2,870	256.5	72.9	0.19	
KSH01A-115-19	10	2,870	(216.2)	89.2	0.24	Unfinished test
KSH01A-115-20	2	2,860	(202.9)	81.2	0.19	Unfinished test

Table 5-2. Calculated mean values and standard deviation. The results in parenthesises in Table 5-1 are excluded in the calculations.

	Density (kg/m^3)	Young's modulus (GPa)	Poisson ratio (–)
Mean value	2,817	76.8	0.21
Standard deviation	37.3	7.6	0.02

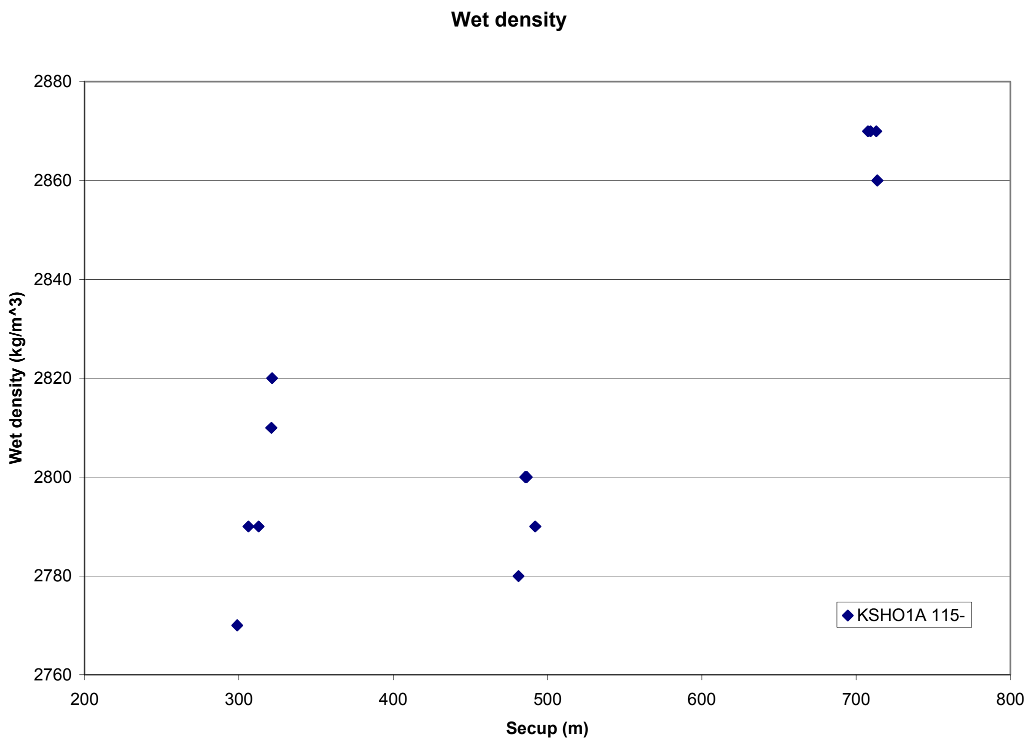

Figure 5-1. Density versus depth at which the samples are taken in the borehole.

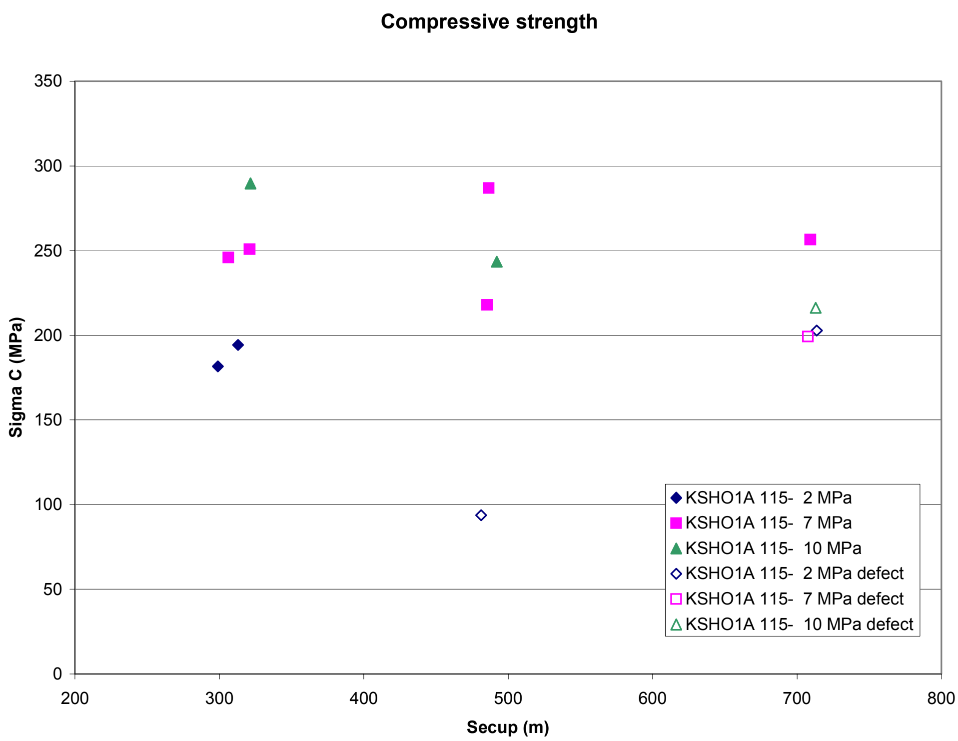

Figure 5-2. Compressive strength versus depth at which the samples are taken in the borehole.

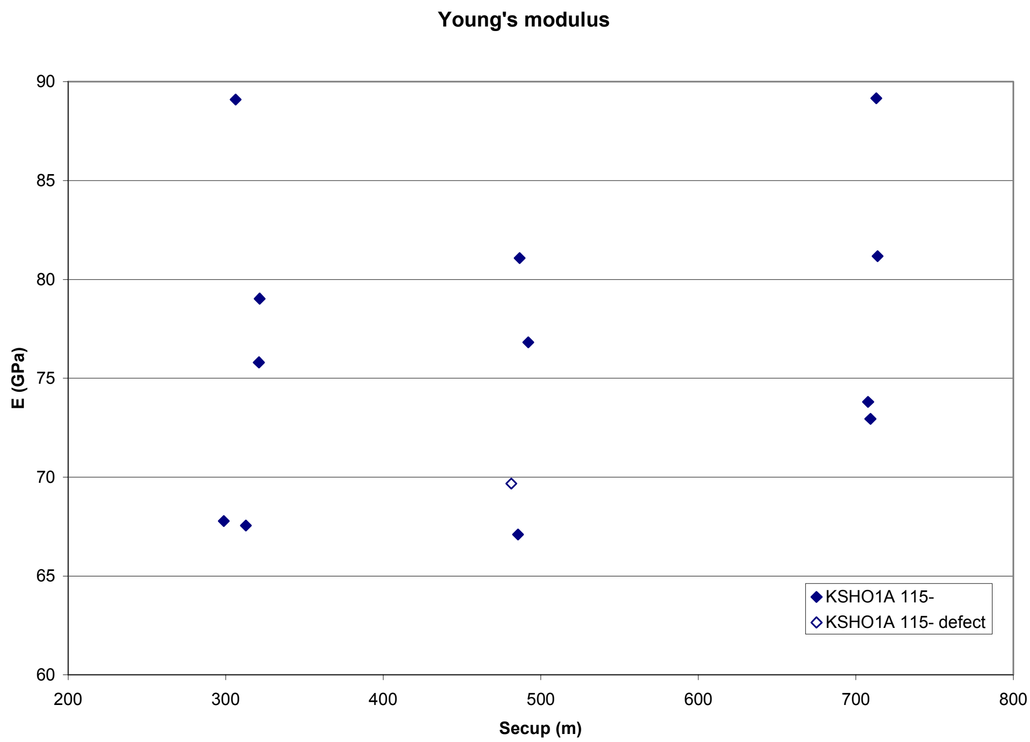

Figure 5-3. *Tangent Young's modulus versus depth at which the samples are taken in the borehole.*

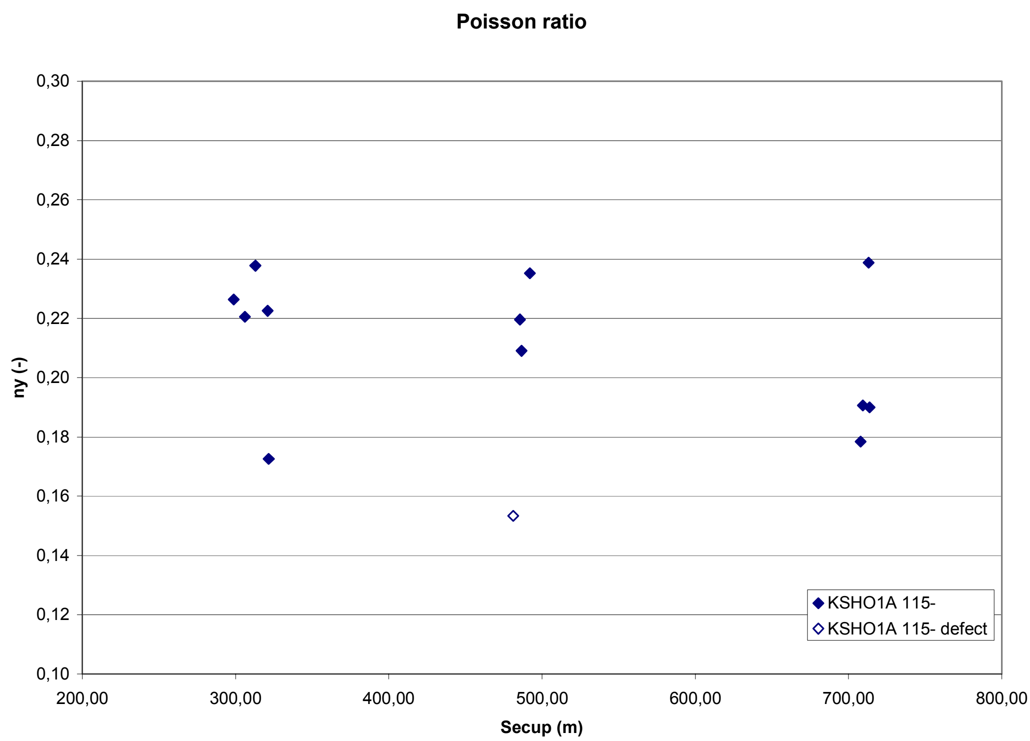

Figure 5-4. *Tangent Poisson ratio versus depth at which the samples are taken in the borehole.*

5.3 Discussion

The testing was conducted according to the method description except for two deviations. It was observed that there was an error in the calibration of the LVDTs at the time for the testing. The LVDTs were therefore recalibrated and a correction of the measured data could be made. This implied that axial and circumferential strains have been determined within an accuracy of 2.7%, which is larger than what is specified in the ISRM-standard /1/. Further, one test (KSH01A-115-20) was restarted after a large sudden expansion leading to a complete unloading of the deviatoric stress. This in was done in order to see if the fracturing process could be driven further. The specimen had only very small residual strength left and the test was stopped.

The activity plan was followed with one exception. Specimen KSH01A-115-16 (Secup 705.08 m) had a visible crack and was replaced by specimen number KSH01A-115-20 (Secup 713.70 m).

References

/1/ **ISRM, 1999.** Draft ISRM suggested method for the complete stress-strain curve for intact rock in uniaxial compression. Int. J. Rock. Mech. Min. Sci. 36(3), pp. 279–289.

/2/ **Martin C D, Chandler N A, 1994.** The progressive fracture of Luc du Bonnet granite. Int. J. Rock. Mech. Min. Sci. & Geomech. Abstr. 31(6), pp. 643–659.

/3/ **Eberhardt E, Stead D, Stimpson B, Rea, R S, 1998.** Identifying crack initiation and propagation thresholds in brittle rock. Can. Geotech. J. 35, pp. 222–233.

/4/ **ASTM 4543-01, 2001.** Standard practice for preparing rock core specimens and determining dimensional and shape tolerance.

/5/ **ISRM, 1979.** Suggested Method for Determining Water Content, Porosity, Density, Absorption and Related Properties and Swelling and Slake-durability Index Properties. Int. J. Rock. Mech. Min. Sci. & Geomech. Abstr. 16(2), pp. 141–156.

/6/ **SS-EN 13755.** Natural stone test methods – Determination of water absorption at atmospheric pressure.

/7/ **ISRM, 1983.** Suggested method for determining the strength of rock material in triaxial compression: Revised version. Int. J. Rock. Mech. Min. Sci. & Geomech. Abstr. 20(6), pp. 283–290.

/8/ **Stråhle A, 2001.** Definition och beskrivning av parametrar för geologisk, geofysisk och bergmekanisk kartering av berg. SKB R-01-19, Svensk Kärnbränslehantering AB. In Swedish.

/9/ **MATLAB, 2002.** The Language of Technical computing, Version 6.5, MathWorks Inc.

Appendix A

The following equations describe the correct calculation of radial strains when using a circumferential deformation device, see Figure A-1.

$$\varepsilon_r = \frac{\Delta C}{C_i}$$

where

$C_i = 2\pi R_i$ = initial specimen circumference

$$\Delta C = \text{change in specimen circumference} = \frac{\pi \cdot \Delta X}{\sin\left(\frac{\theta_i}{2}\right) + \left(\pi - \frac{\theta_i}{2}\right)\cos\left(\frac{\theta_i}{2}\right)}$$

and

ΔX = change in LVDT reading = $X_i - X_f$

(X_i = initial chain gap; X_f = current chain gap)

$$\theta_i = \text{initial chord angle} = 2\pi - \frac{L_c}{R_i + r}$$

L_c = chain length (measured from center of one end roller to center of other end roller)

r = roller radius

R_i = initial specimen radius

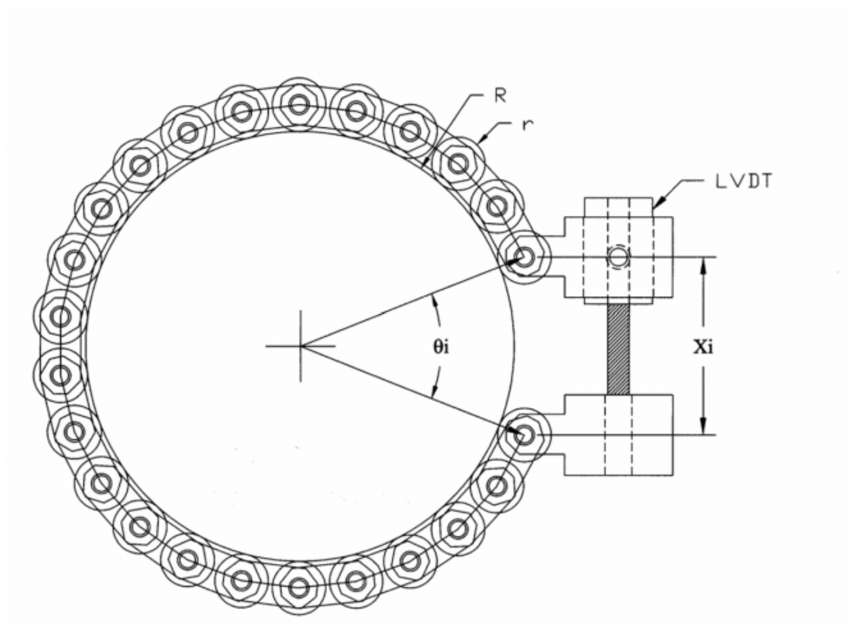

Figure A-1. *Chain for radial deformation measurement.*

Appendix B

This Appendix contains complementary results showing the volumetric strain ε_{vol} versus the axial strain ε_a and the actual radial strain rate $d\varepsilon_r$ /dt versus time. The complementary results for all tests are shown below.

Specimen ID: KSH01A−115−01

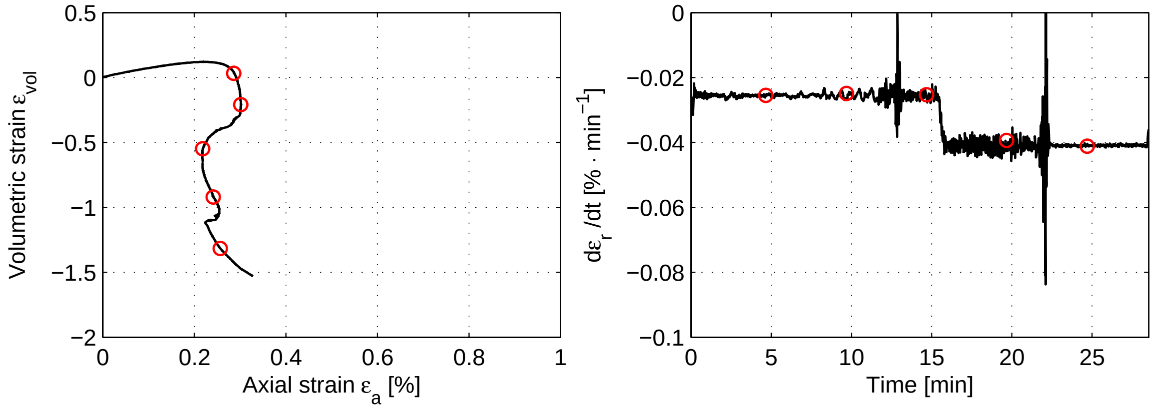

Specimen ID: KSH01A−115−03

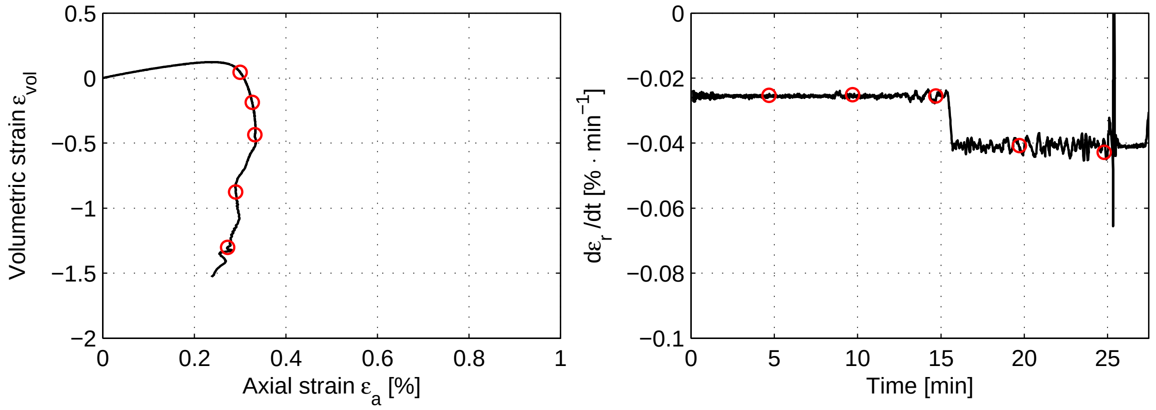

Specimen ID: KSH01A−115−05

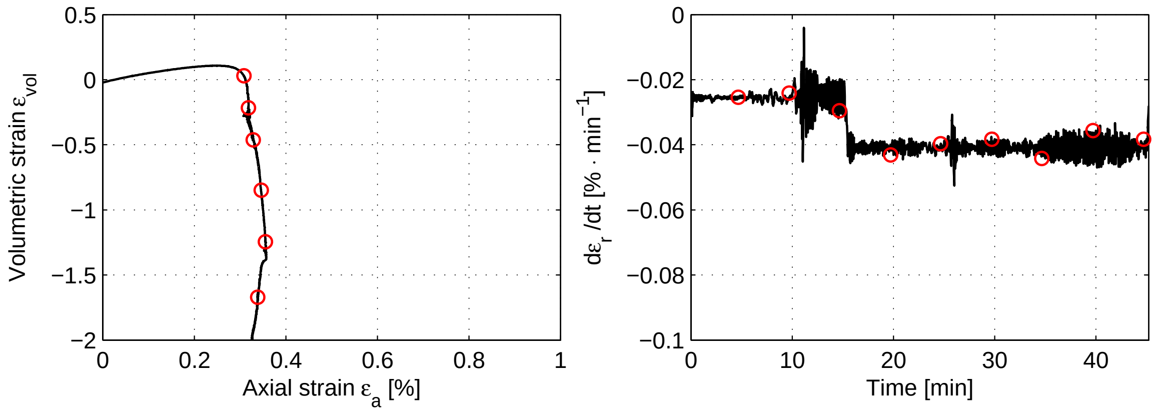

Specimen ID: KSH01A−115−07

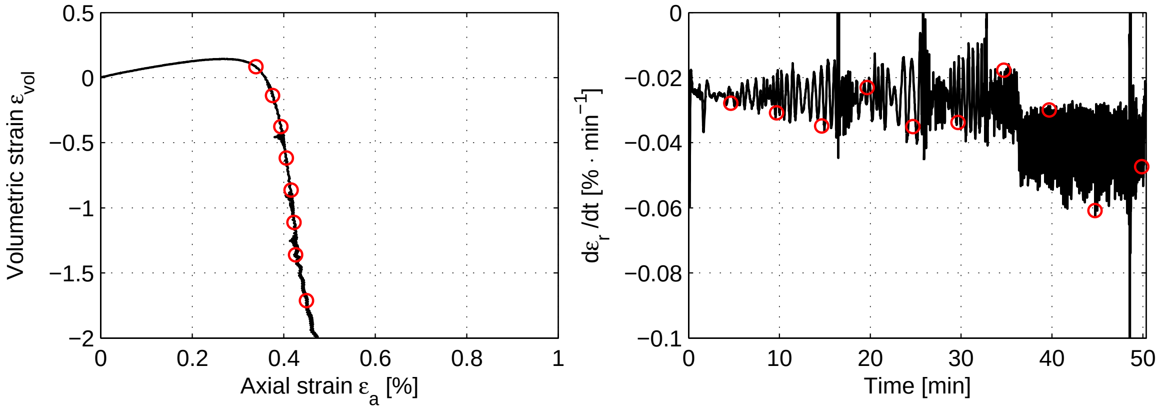

Specimen ID: KSH01A−115−09

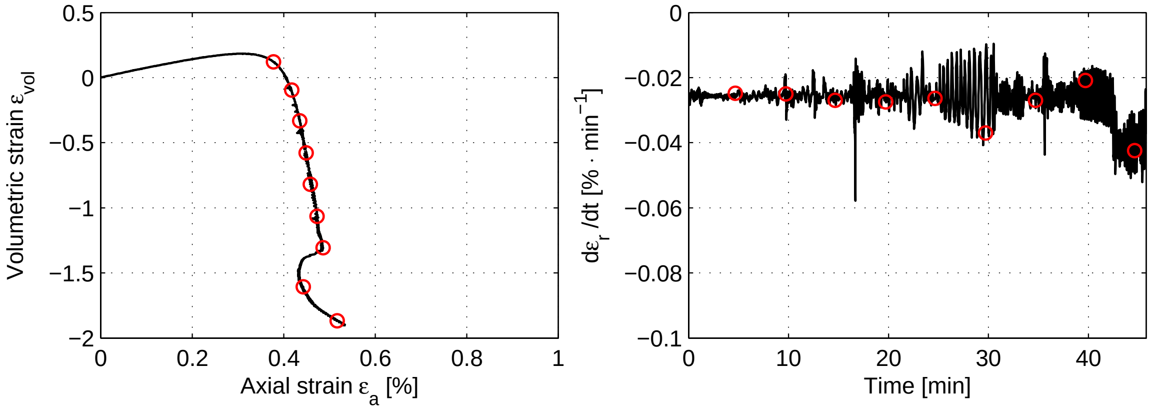

Specimen ID: KSH01A−115−11

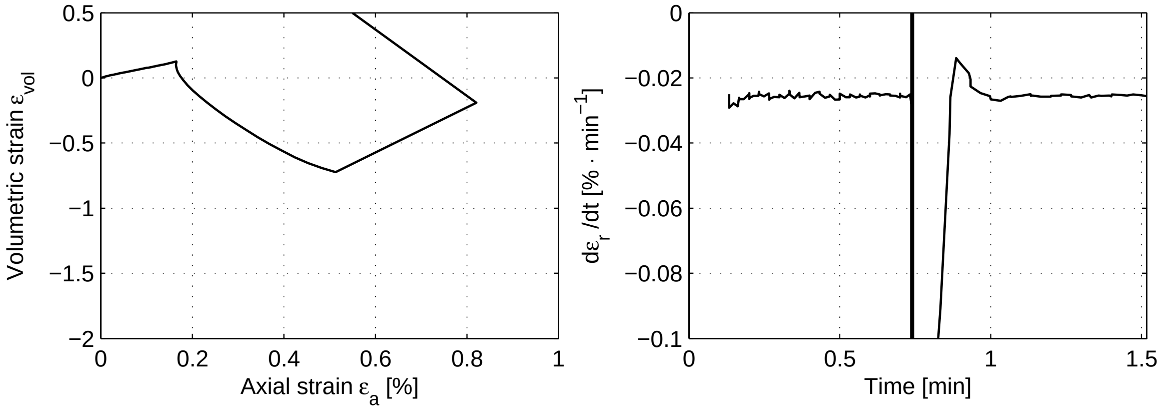

Specimen ID: KSH01A−115−12

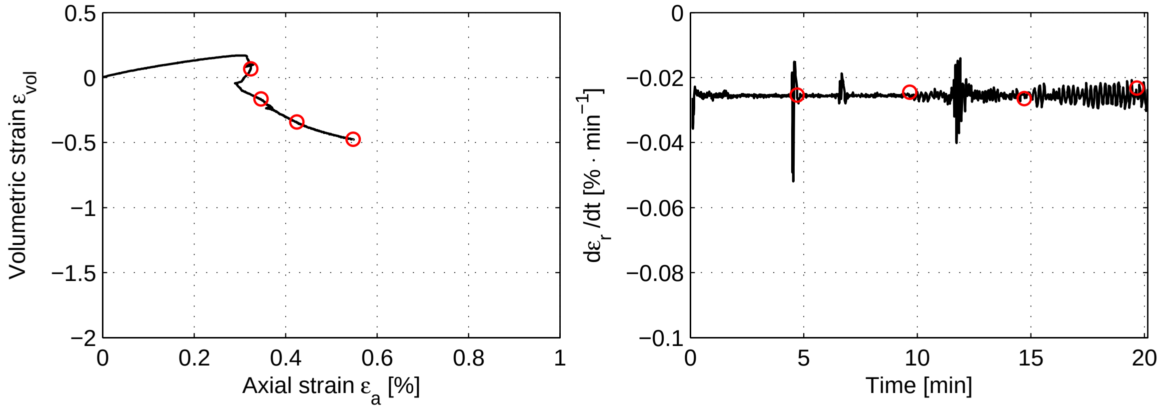

Specimen ID: KSH01A−115−13

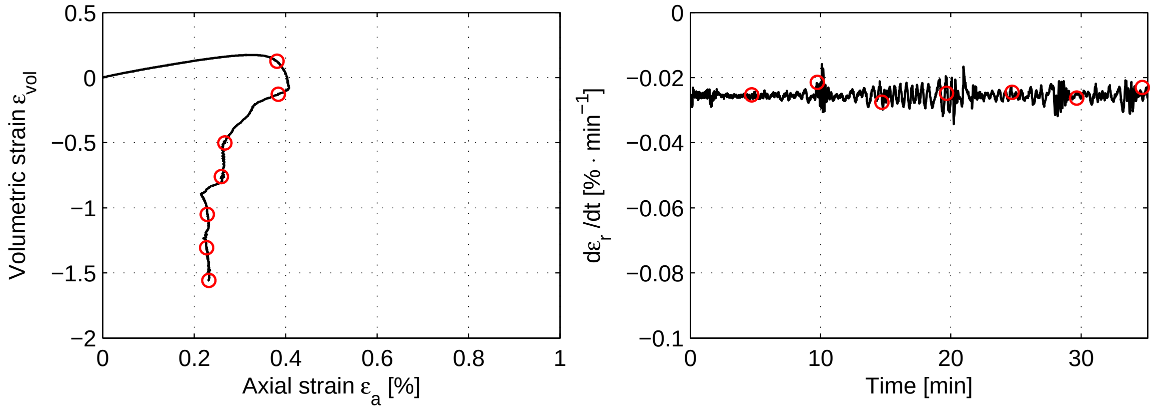

Specimen ID: KSH01A−115−14

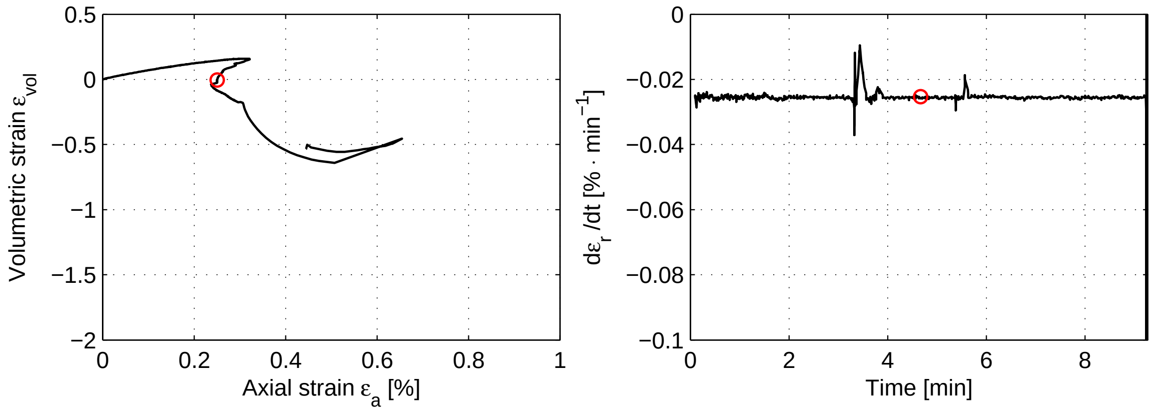

Specimen ID: KSH01A−115−17

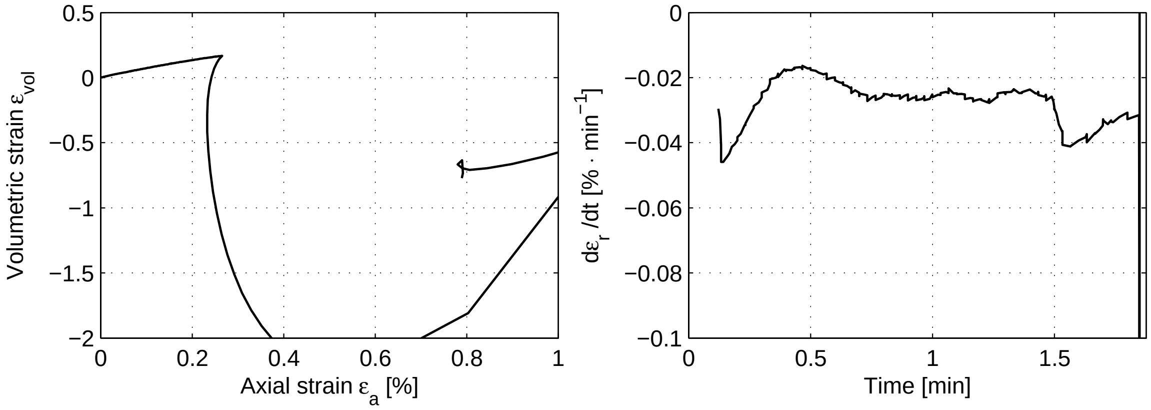

Specimen ID: KSH01A−115−18

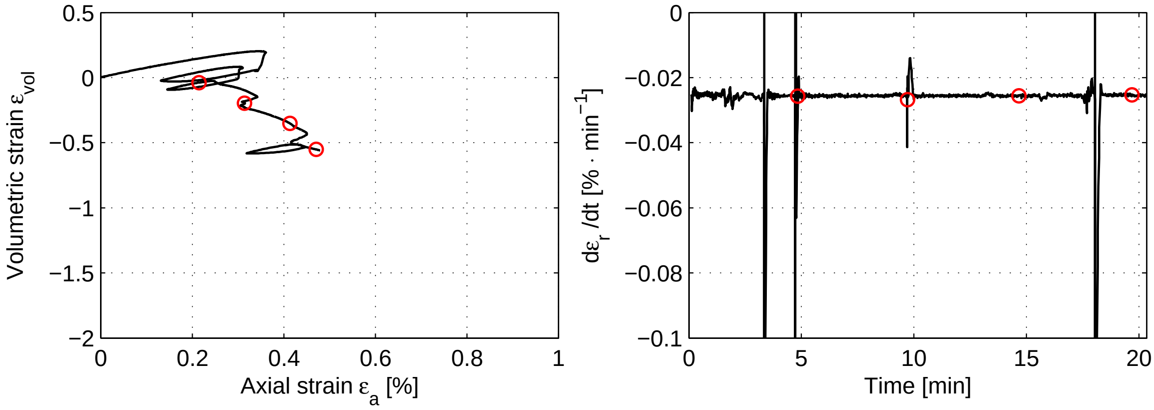

Specimen ID: KSH01A−115−19

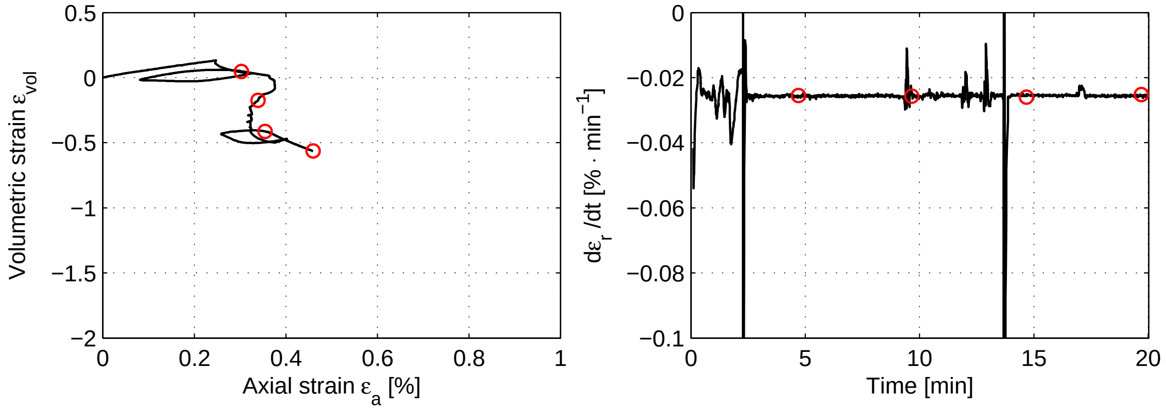

Specimen ID: KSH01A−115−20